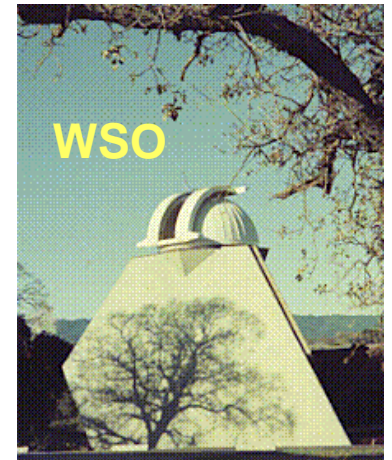


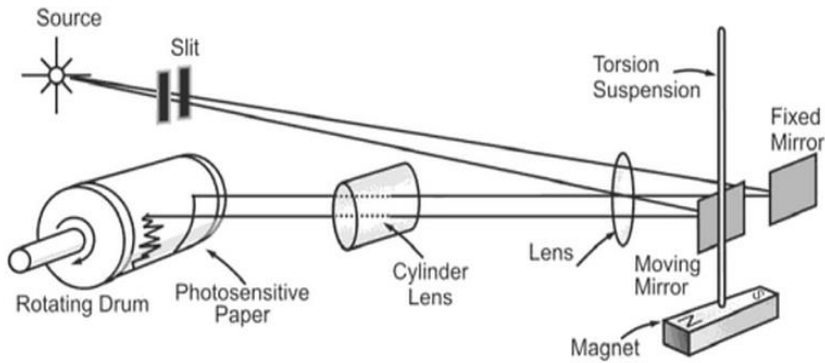
Recent Progress in Long-Term Variability of Solar Activity

Leif Svalgaard

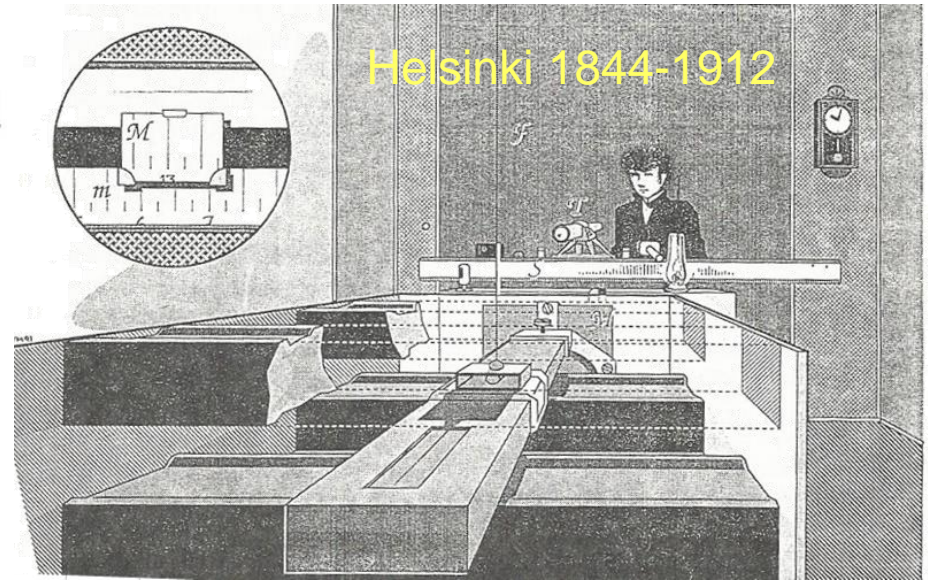
Stanford University, California, USA

Keynote Talk, SCOSTEP-13, Xi'an 西安 , China
13th October, 2014



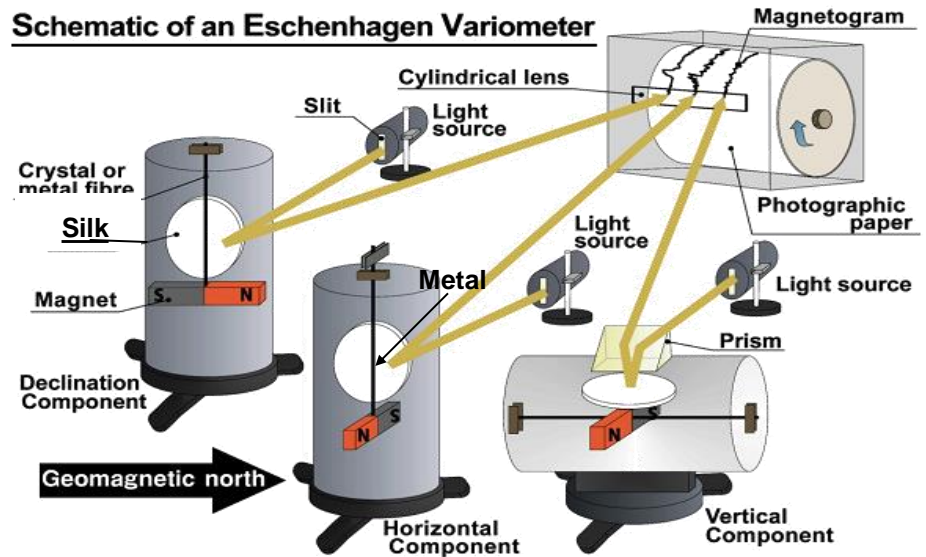


Classic Method since 1846



Instruments ca. 1910

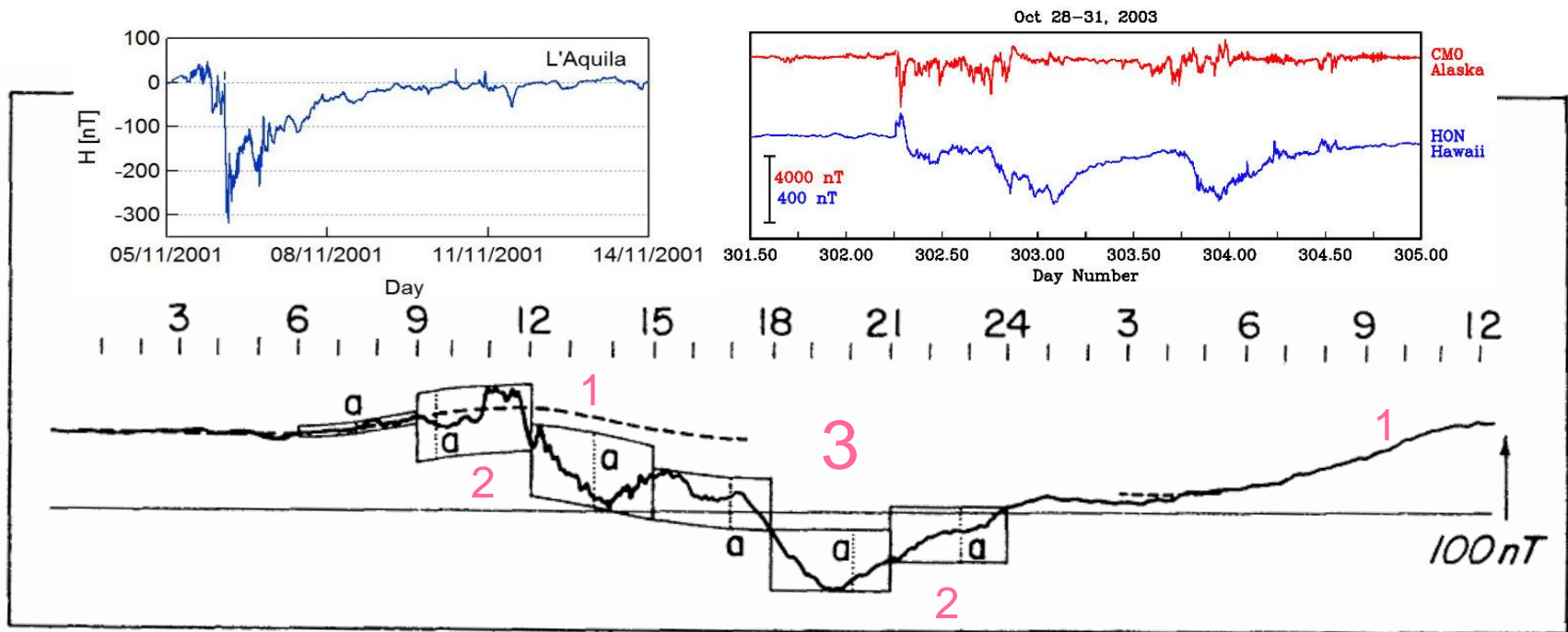
Schematic of an Eschenhagen Variometer



Modern Instrument

Using variation since 1830s of the Earth's Magnetic Field as a measuring device ²

Typical Recording over 36 Hours



Three simultaneous features:

1: A Regular Daily Variation [it took ~200 years to figure out the cause]

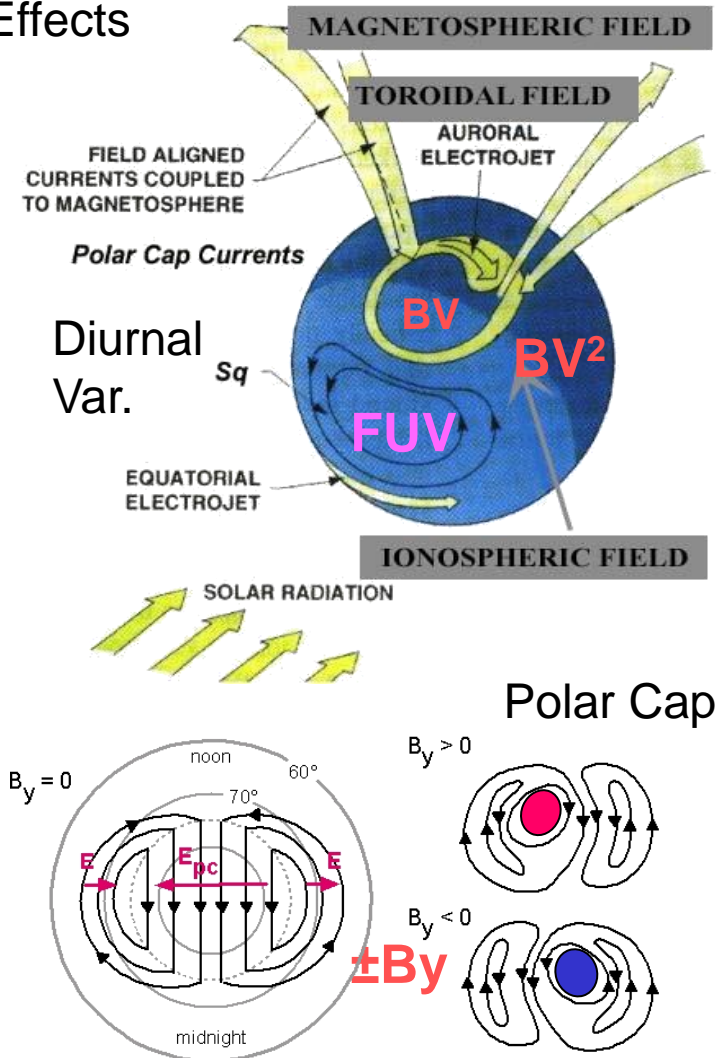
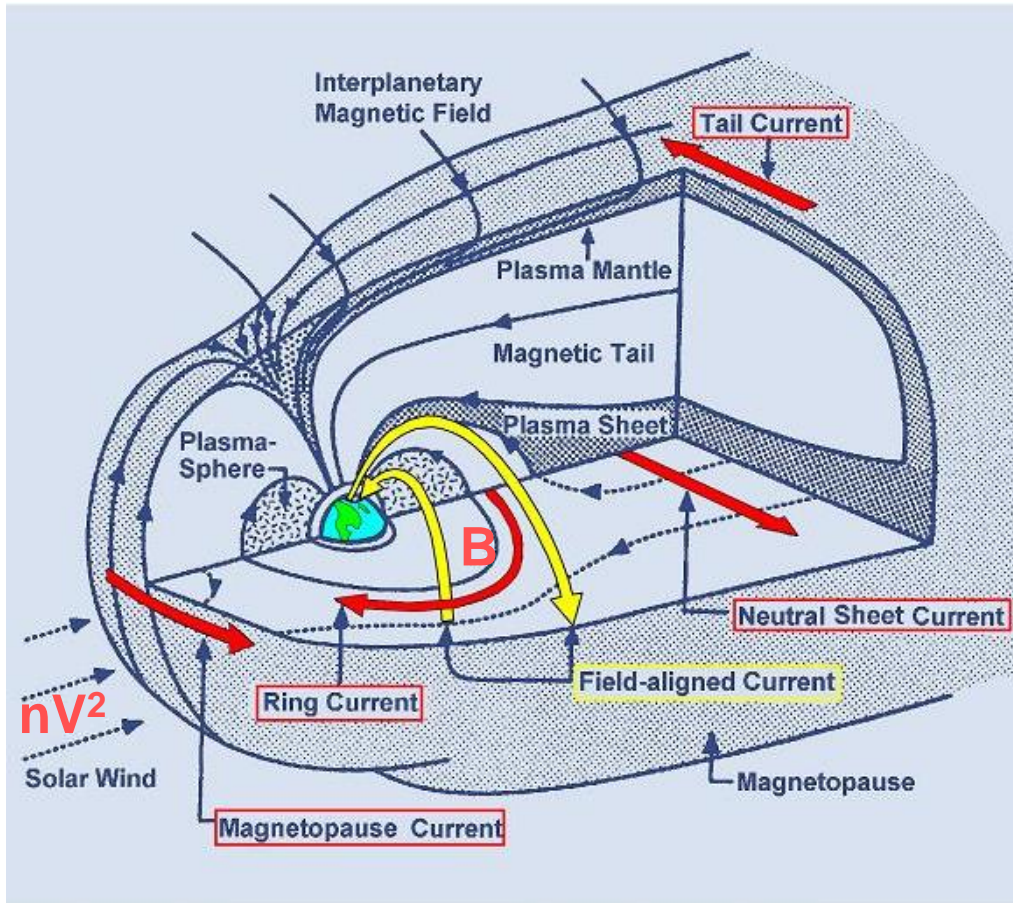
2: Shorter-term [~3 hour] fluctuations ['substorms' recognized in 1960s]

3: Large disturbances ['geomagnetic storms' explained in the 1930-1960s]

The complicated, simultaneous effects withstood understanding for a long time

Electric Current Systems in Geospace

Different Current Systems \longleftrightarrow Different Magnetic Effects

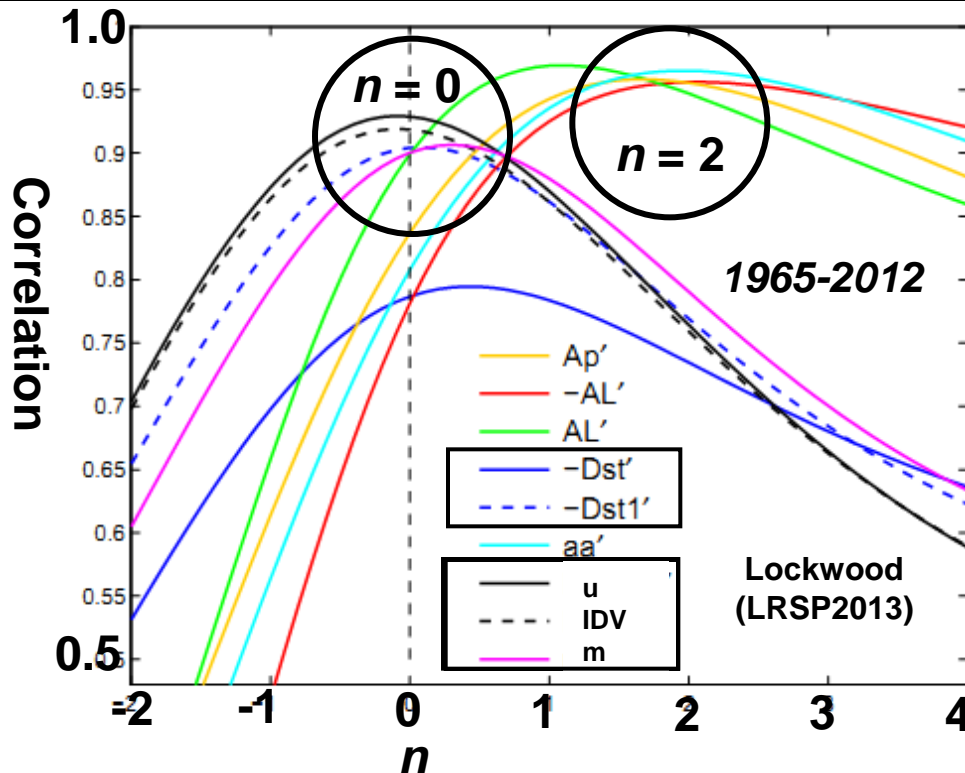
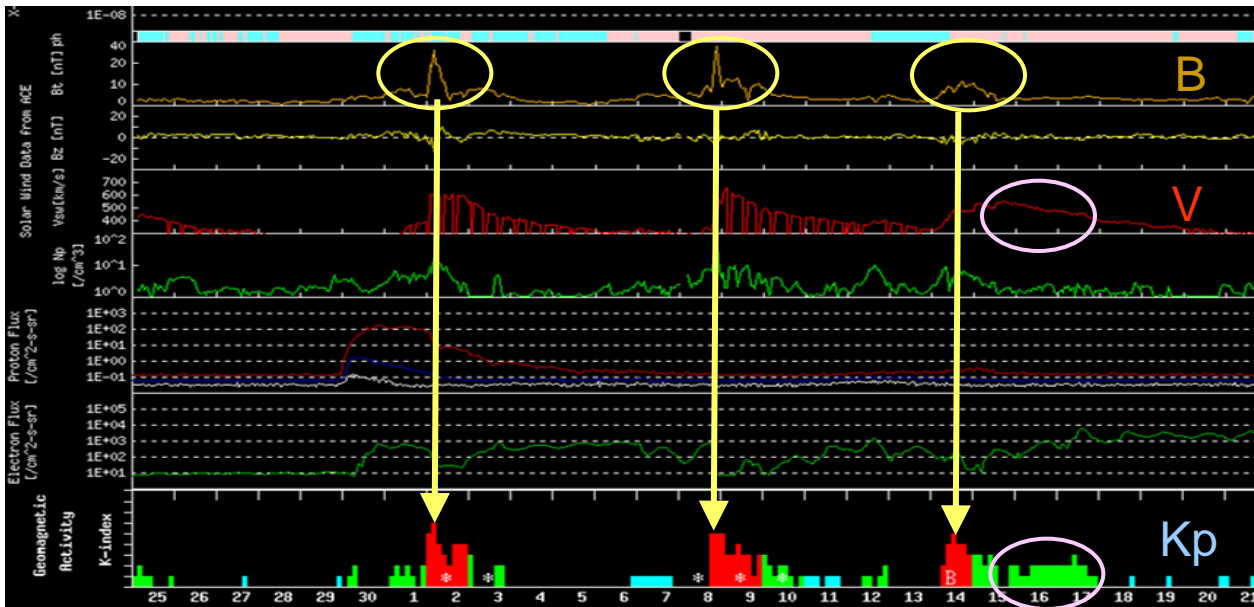


We can now invert the Solar Wind – Magnetosphere relationships...

'Different Strokes for Different Folks'

- The key to using geomagnetism to say something about the sun is the realization that geomagnetic 'indices' can be constructed that respond differently to different solar and solar wind parameters, so can be used to disentangle the various causes and effects
- The IDV [Interdiurnal Variability Index] and Dst measure the strength of the Ring Current
- The IHV [Interhourly Variability Index] and aa/am/ap measure the strength of the auroral electrojets [substorms]
- The PCI [Polar Cap Index] measures the strength of the Cross Polar Cap current
- The Sq current system measures the strength of the solar EUV flux
- The Svalgaard-Mansurov Effect measures the polarity of the Solar Wind Magnetic Field
- In the last decade of research this insight (e.g. Svalgaard et al. 2003) has been put to extensive use and a consensus is emerging

27-day Bartels Rotation showing B and Kp peaks



Correlation between
Heliospheric BV^n and
several geomagnetic
indices as a function of n

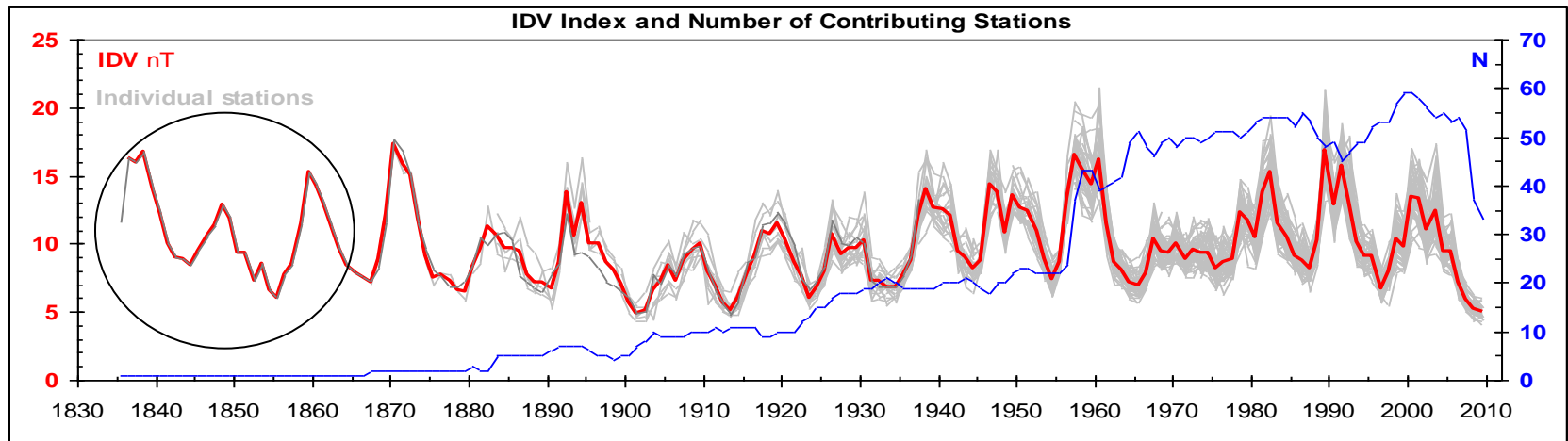
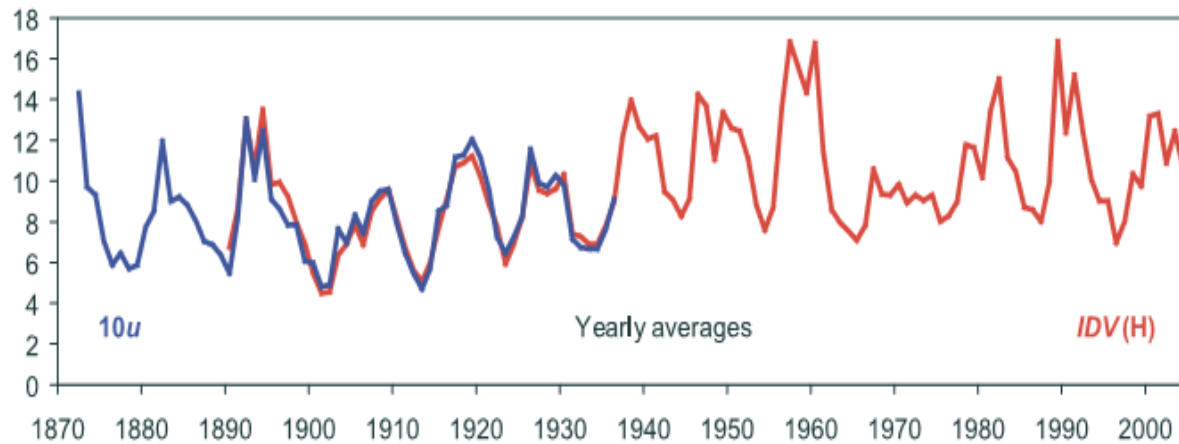
The IDV and Dst indices thus
depend on B only ($n = 0$).

Substorm indices [e.g. aa
and IHV] depend on BV^2

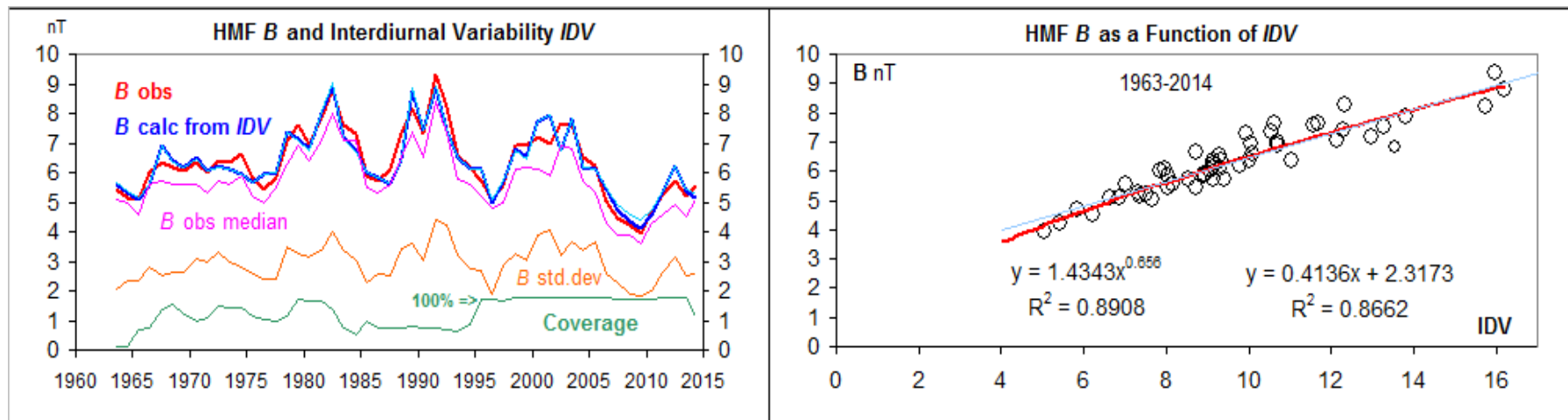
Bartels' u -measure and our IDV -index

u : all day |diff|,
1 day apart

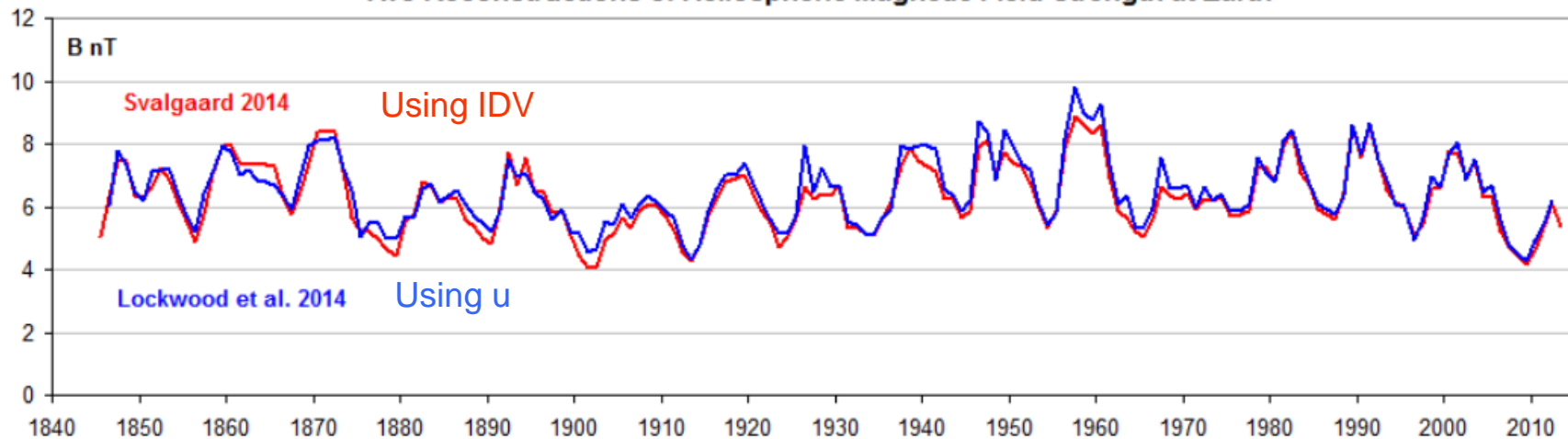
IDV : midnight
hour |diff|,
1 day apart



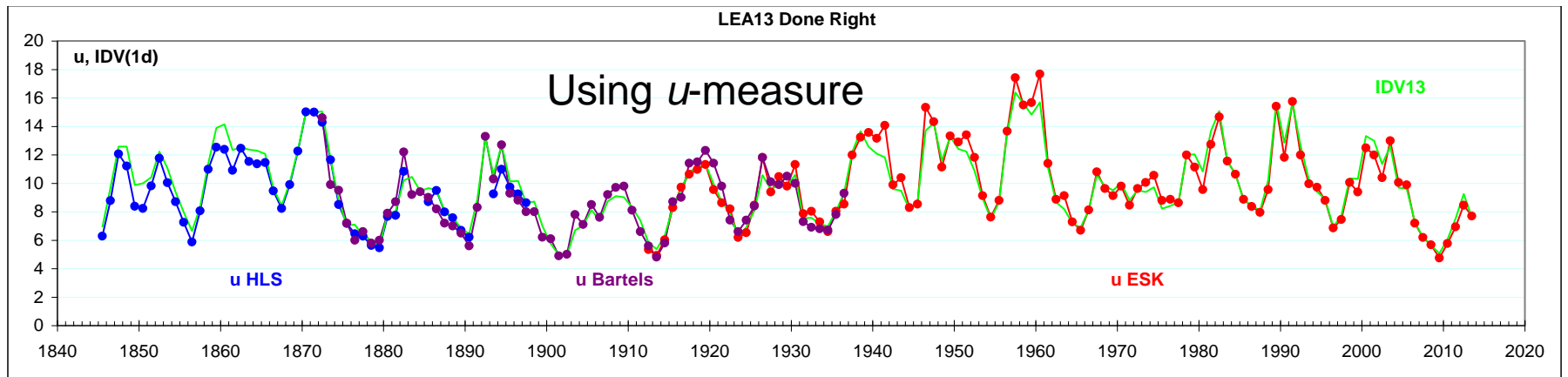
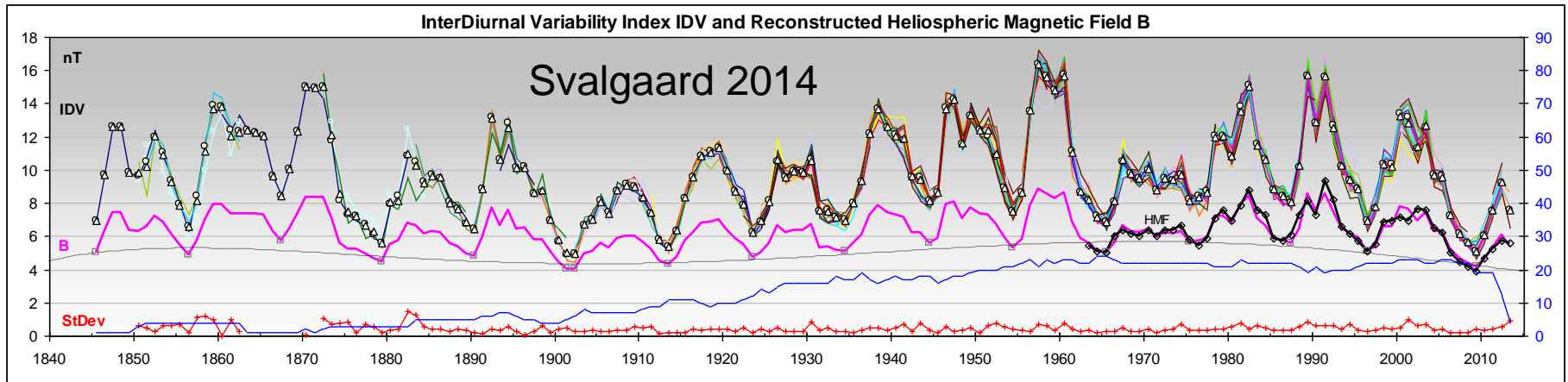
Different Groups have now Converged on a Consensus of HMF B near Earth



Two Reconstructions of Heliospheric Magnetic Field Strength at Earth

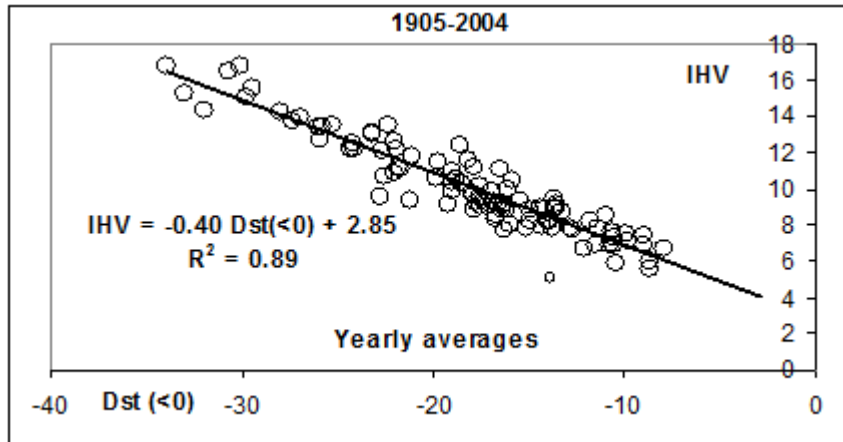


Progress in Reconstructing Solar Wind Magnetic Field back to 1840s

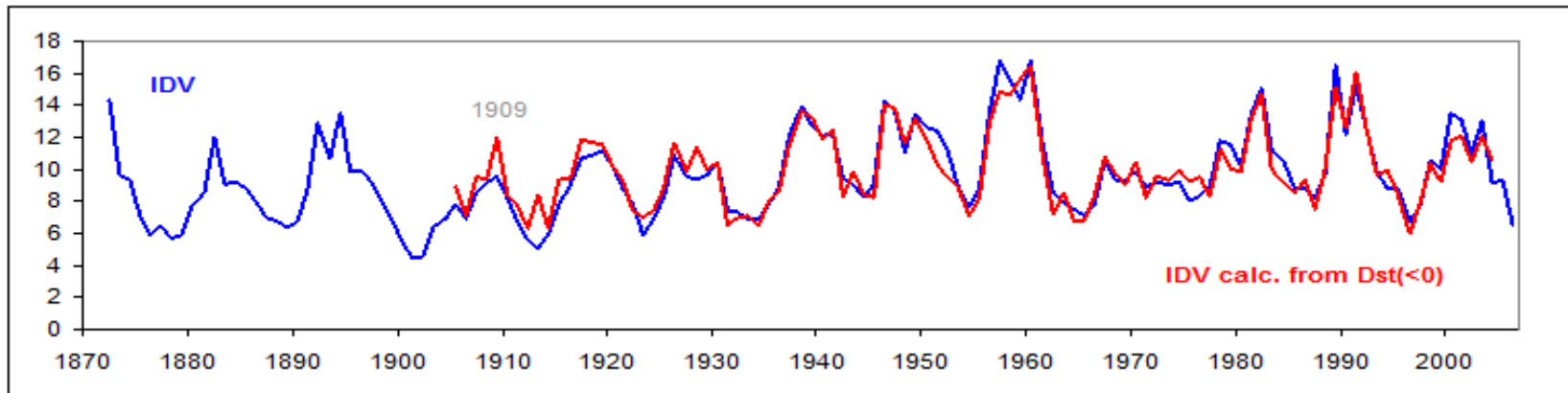


Even using only ONE station, the 'IDV' signature is strong enough to show the effect

IDV measures the same as the Negative part of Dst Index

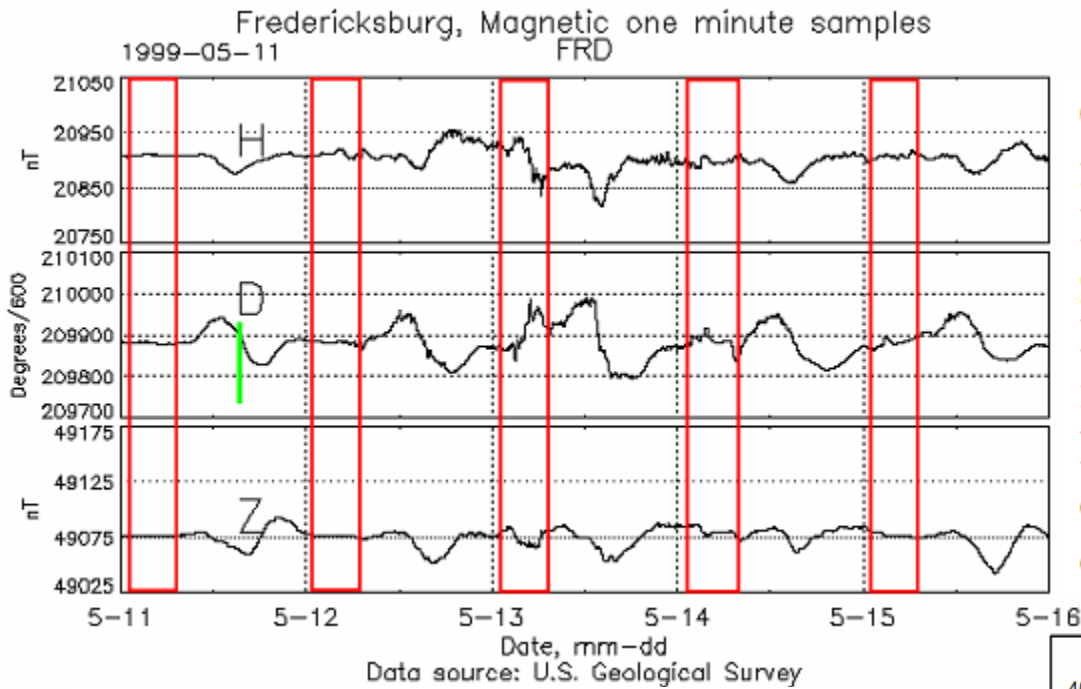


Coronal Mass Ejections (CMEs) add (closed) magnetic flux to the IMF. CMEs hitting the Earth create magnetic storms feeding energy into the inner magnetosphere (“ring current”). The Dst-index is aimed at describing this same phenomenon, but only the negative contribution to Dst on the nightside is effectively involved. We therefore expect (negative) Dst and IDV to be strongly related, and they are

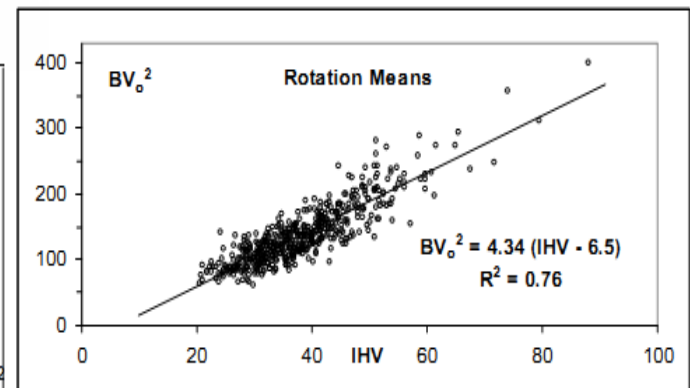
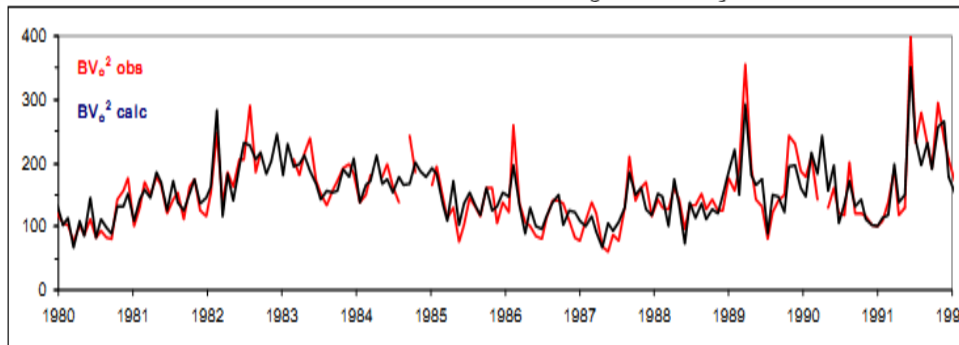


We used a derivation of Dst by J. Love back to 1905. Similar results are obtained with the Dst series by Mursula et al. (to 1932) or with the “official” Dst series (to 1957). The very simple-to-derive IDV series compares favorably with the much more elaborate $Dst(<0)$.

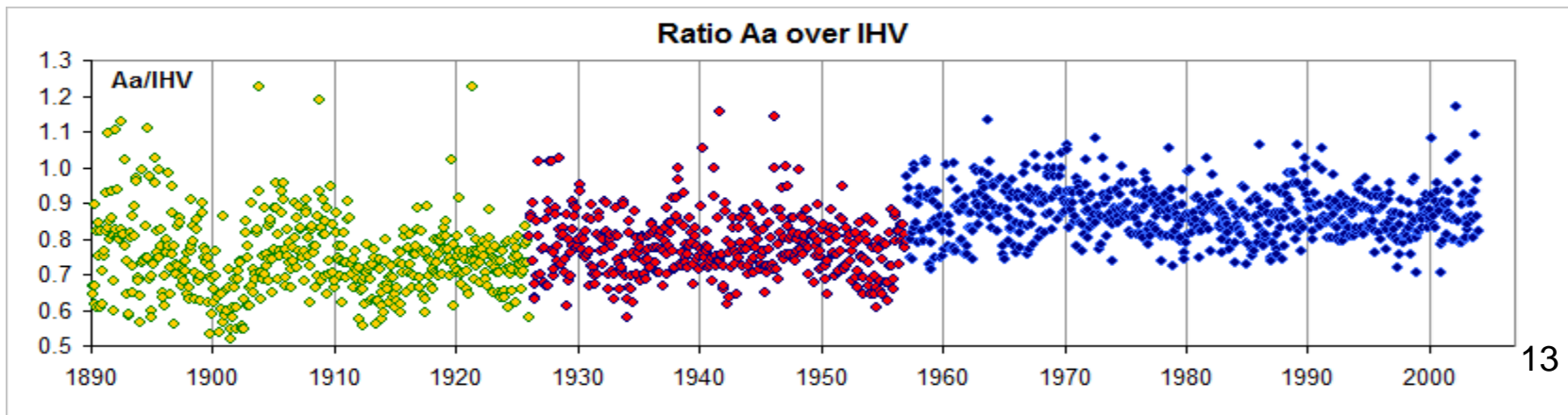
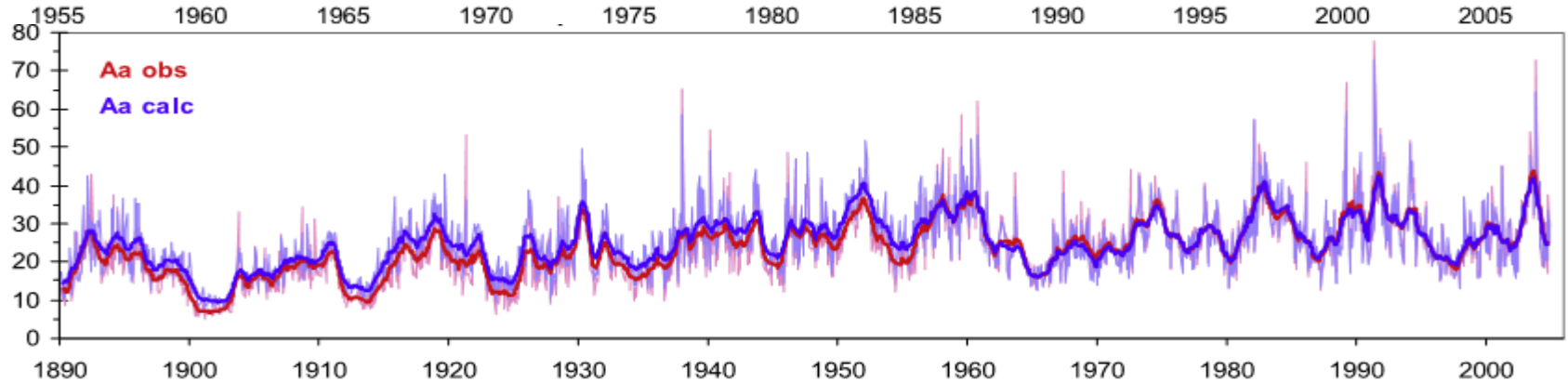
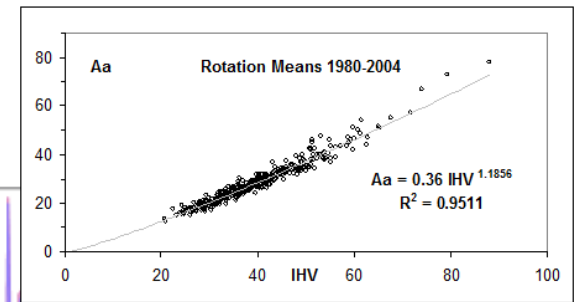
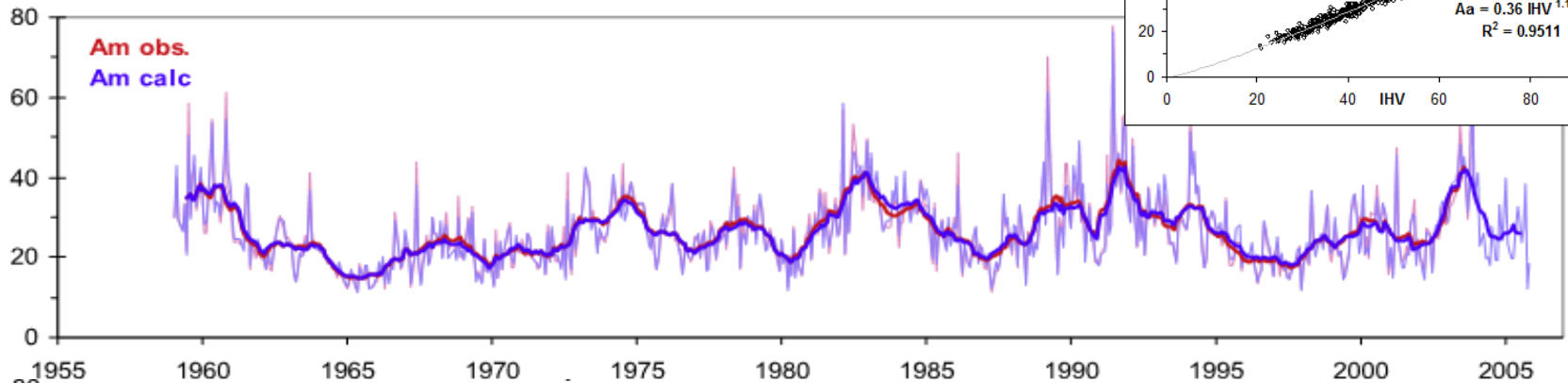
The *IHV* Index gives us BV^2



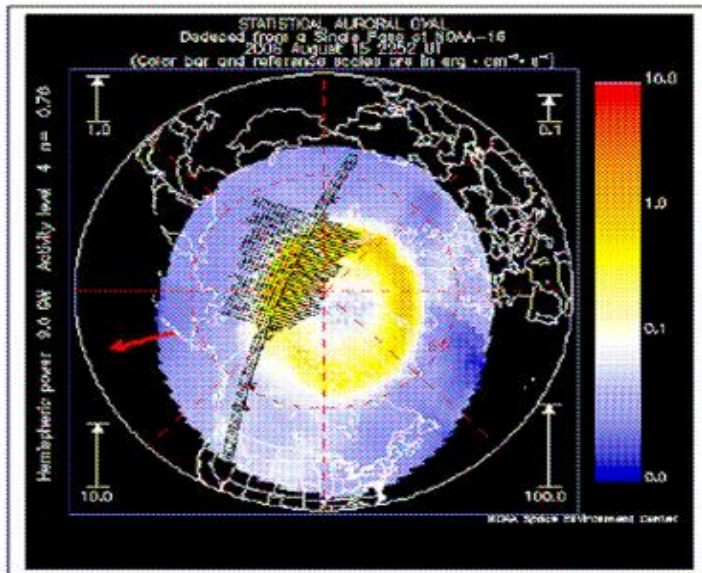
Calculating the variation (sum of unsigned differences from one hour to the next) of the field during the night hours [red boxes] from simple hourly means (the Interhourly Variation) gives us a quantity that correlates with BV^2 in the solar wind



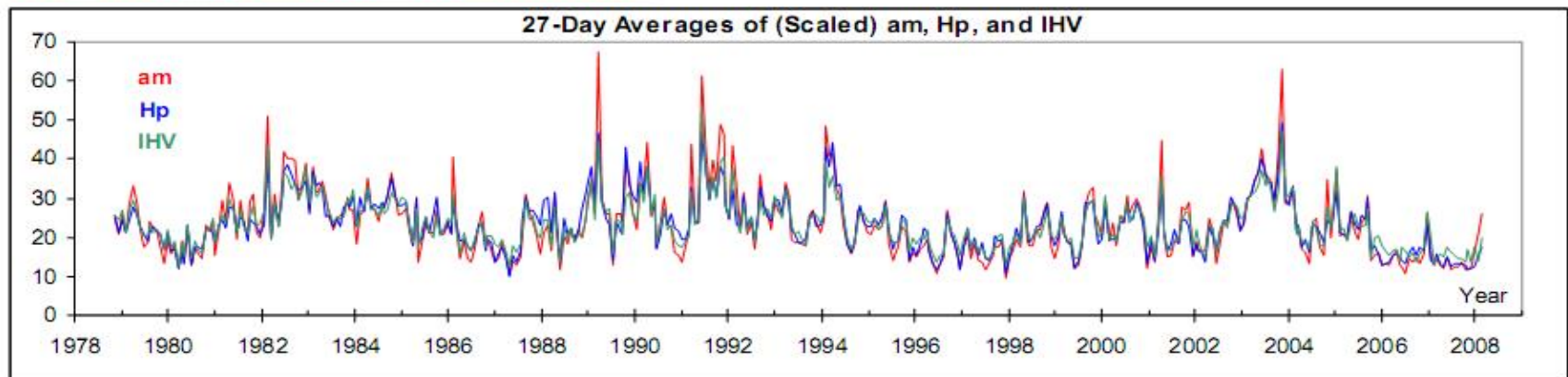
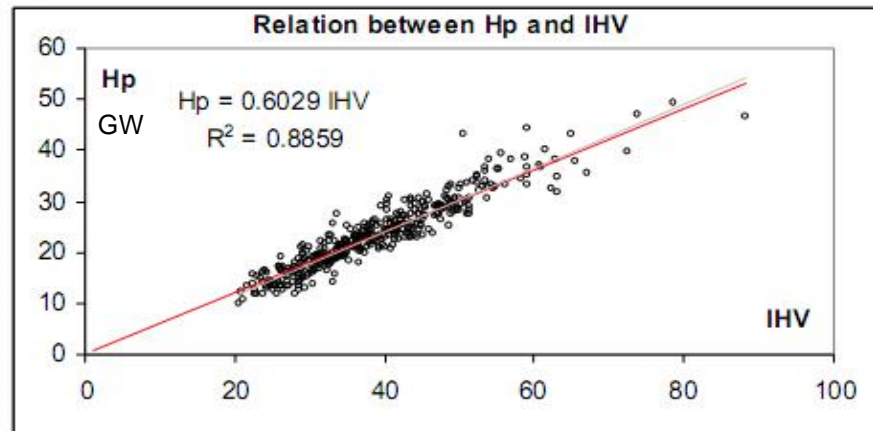
We can calculate Am [and Aa] from IHV



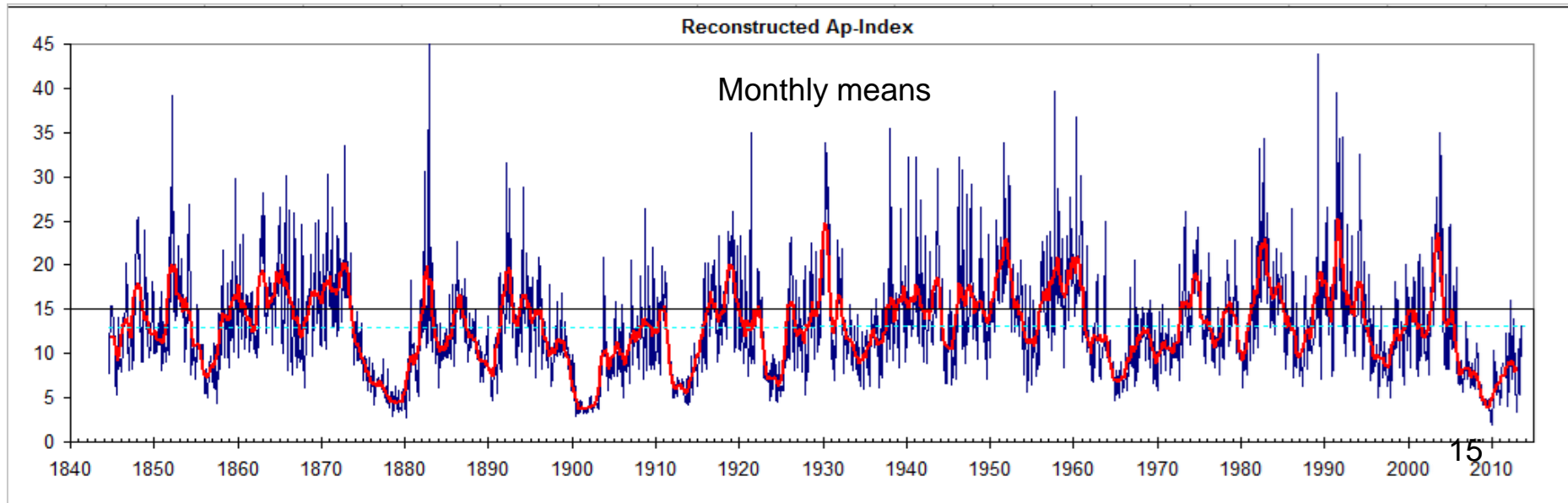
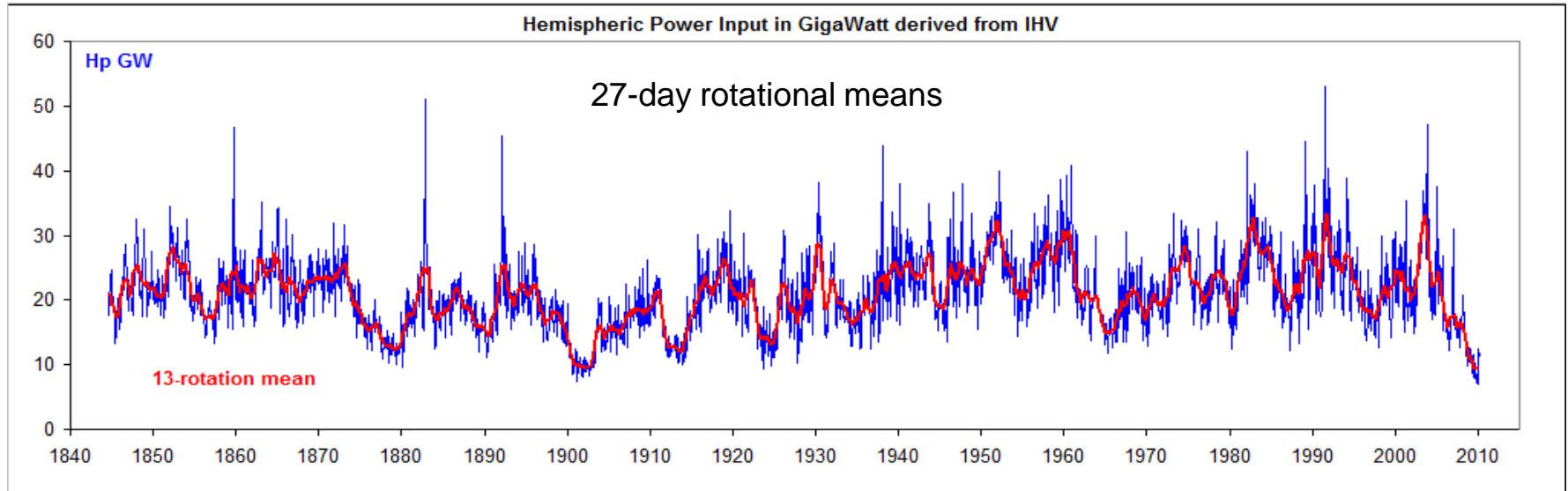
IHV is a Measure of Power Input [in GW] to the Ionosphere (Measured by POES)



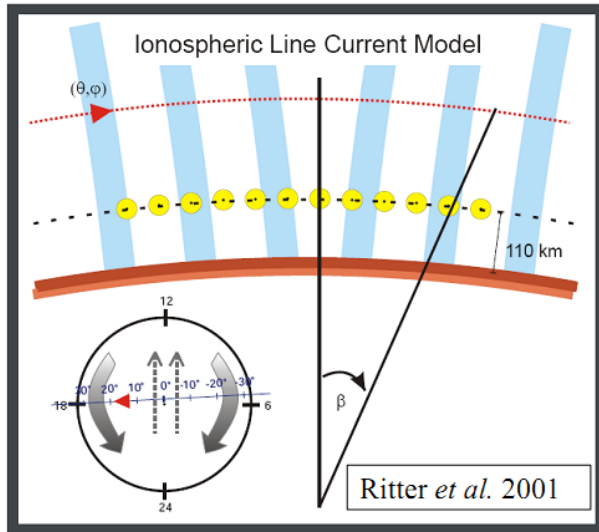
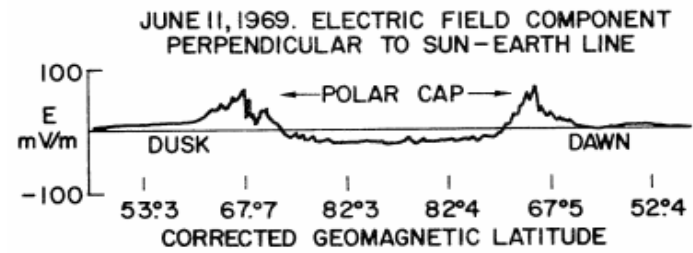
IHV is directly proportional to the power input (*Hp*) to the upper atmosphere:



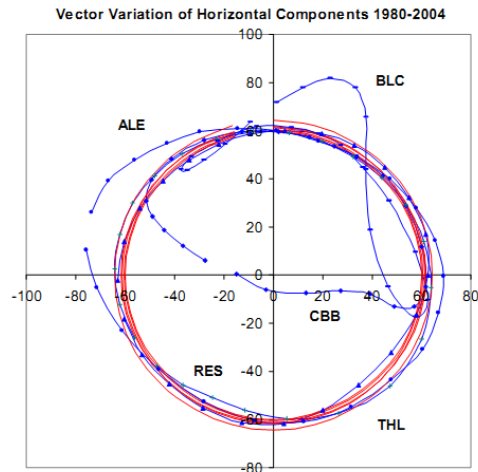
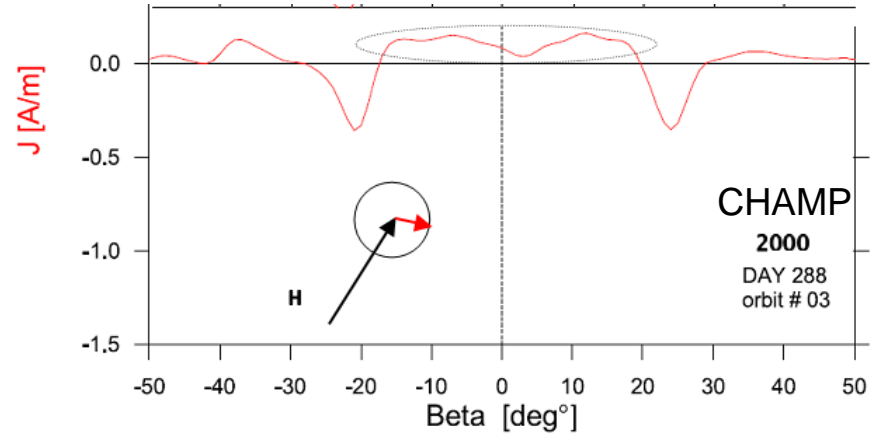
We can thus get H_p [and also A_p , for people who are more familiar with that] back to the 1840s



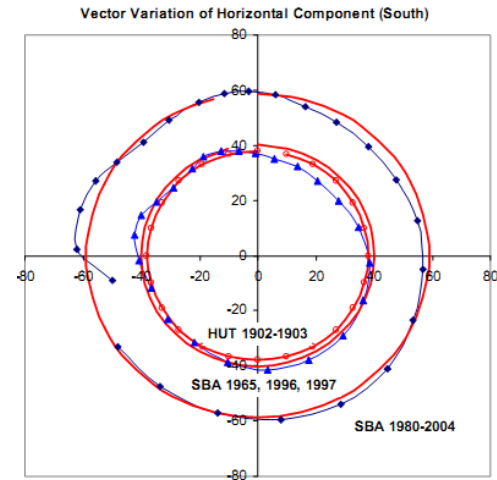
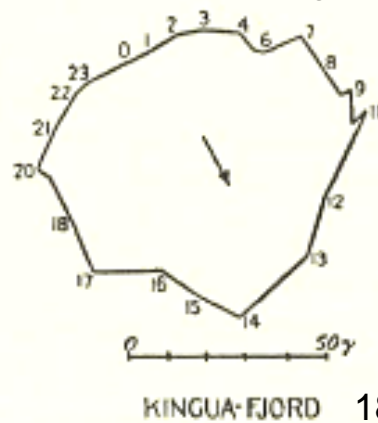
Cross Polar Cap Hall Current



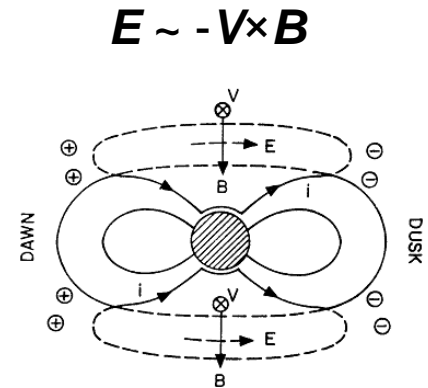
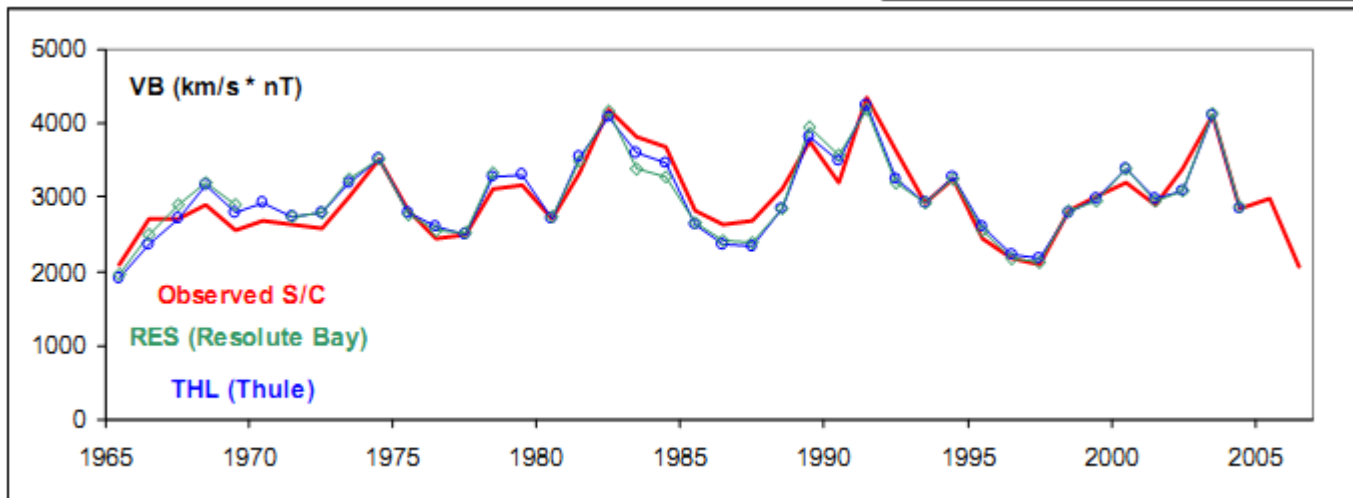
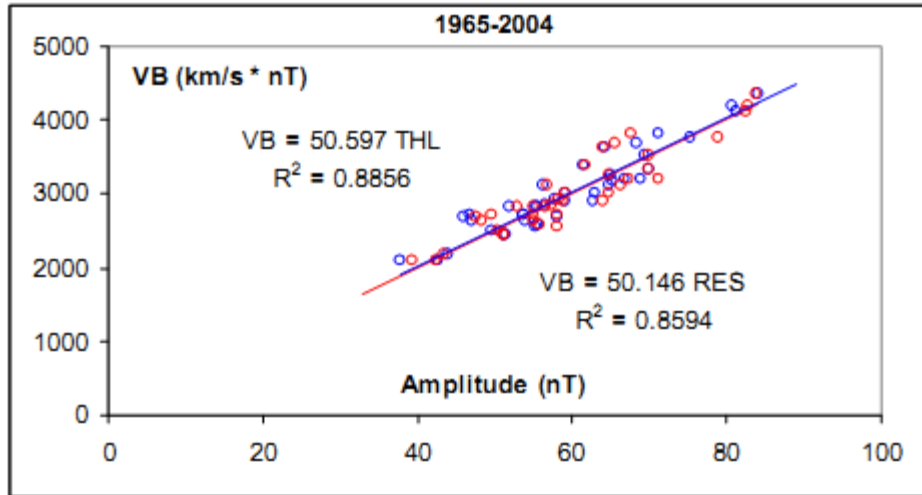
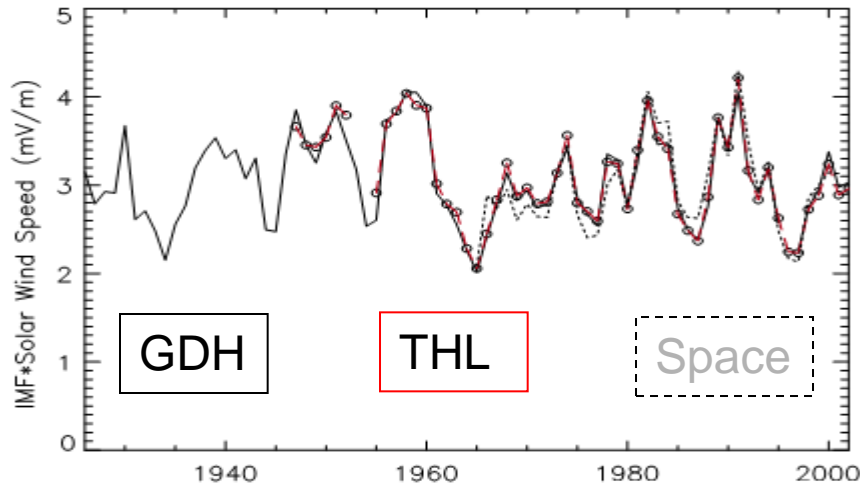
Ionospheric Hall Current across Polar Cap



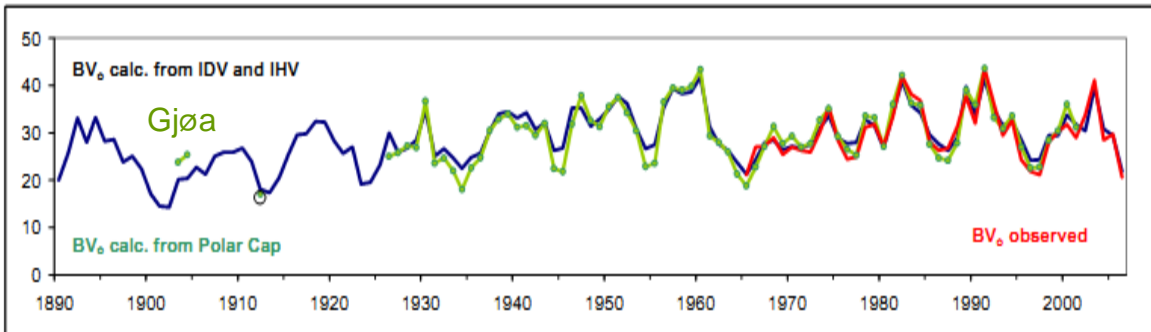
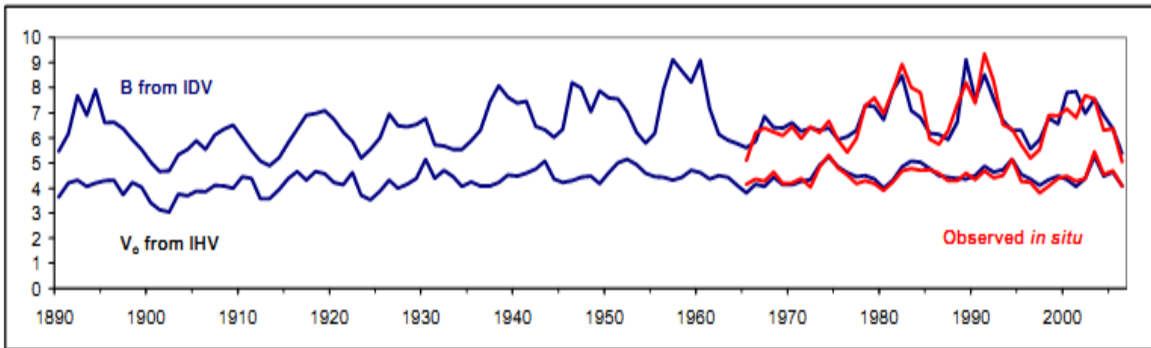
Been known a long time:



Cross Polar Cap Potential Drop



Overdetermined System: 3 Eqs, 2 Unknowns

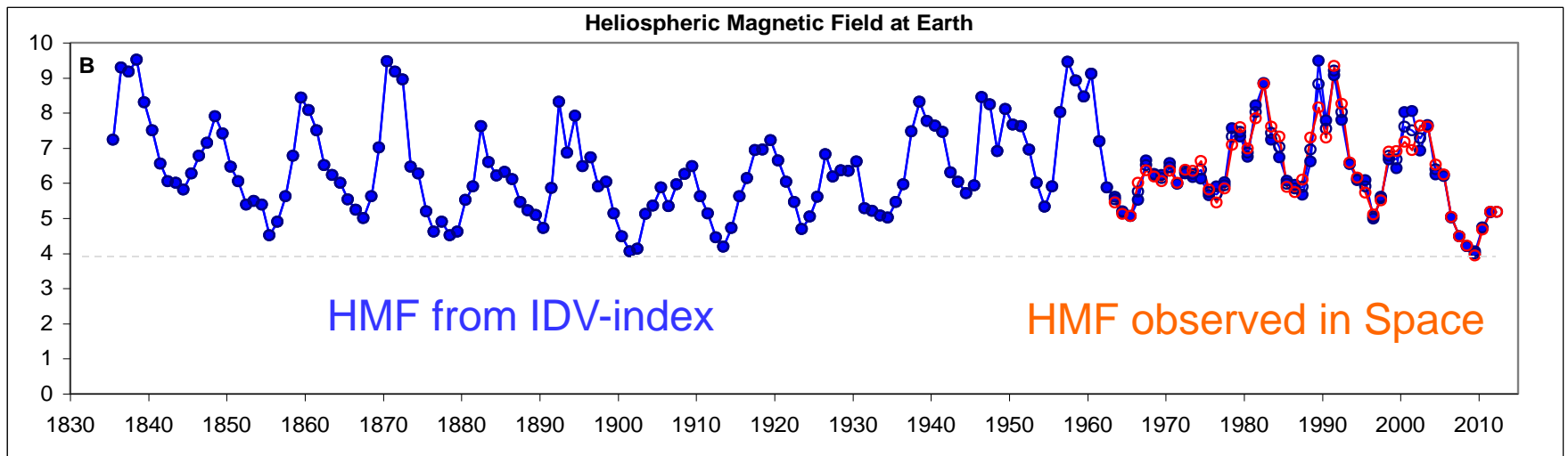


$$B = p \text{ (IDV)}$$

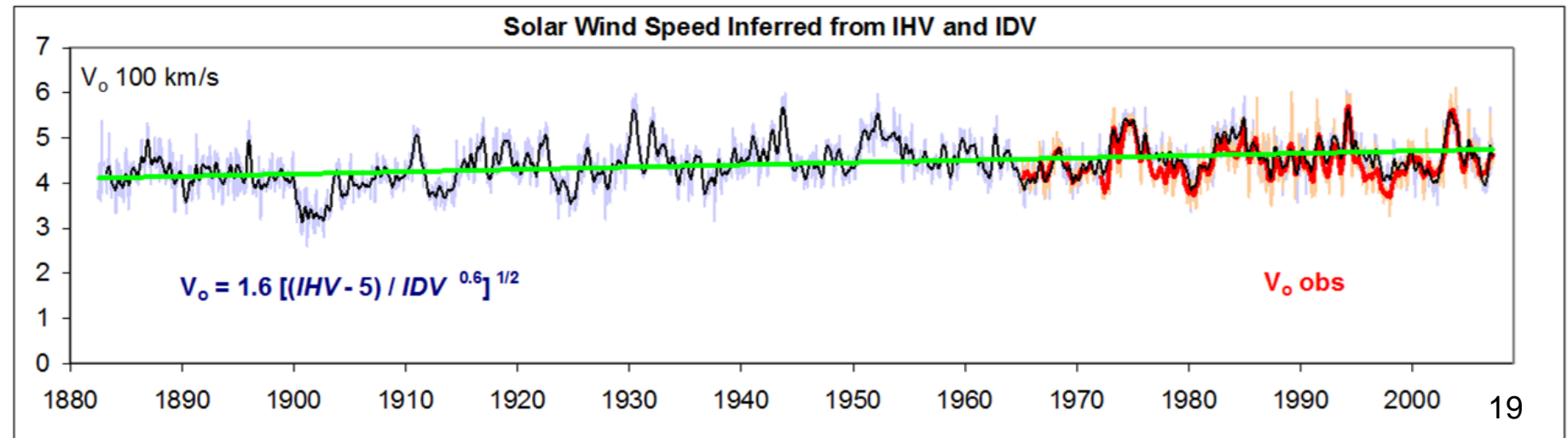
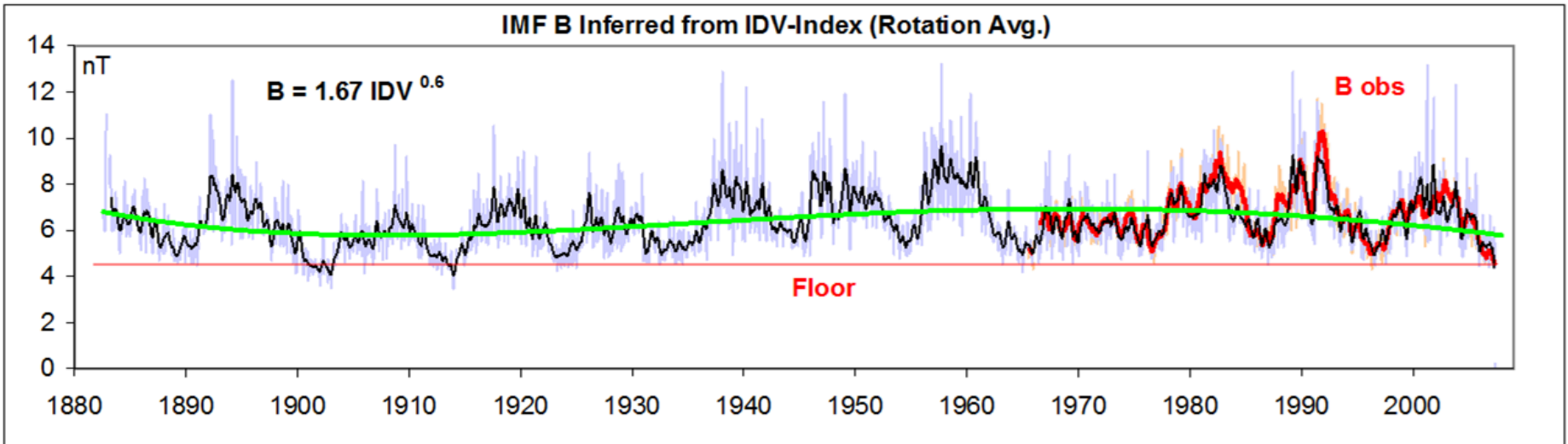
$$BV^2 = q \text{ (IHV)}$$

$$VB = r \text{ (PCap)}$$

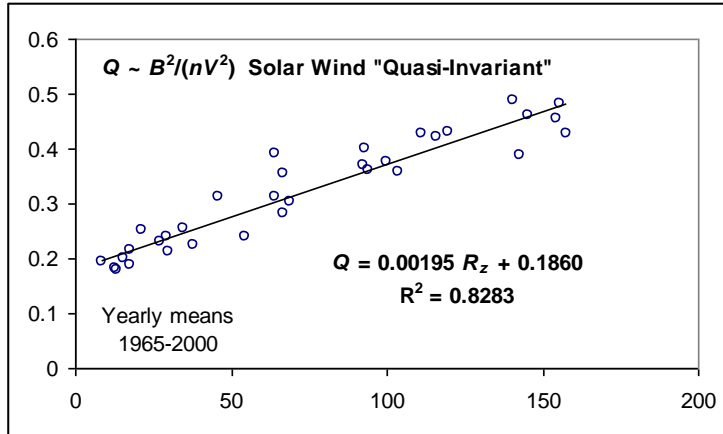
Here is B back to the 1830s:



We can even reconstruct HMF B and Solar Wind V on a 27-day basis



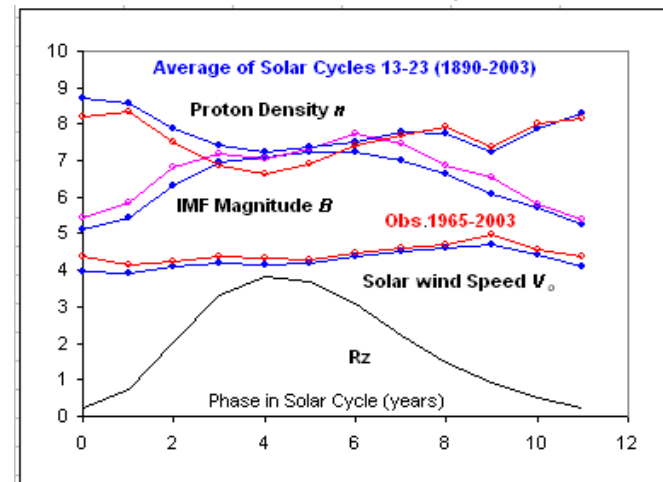
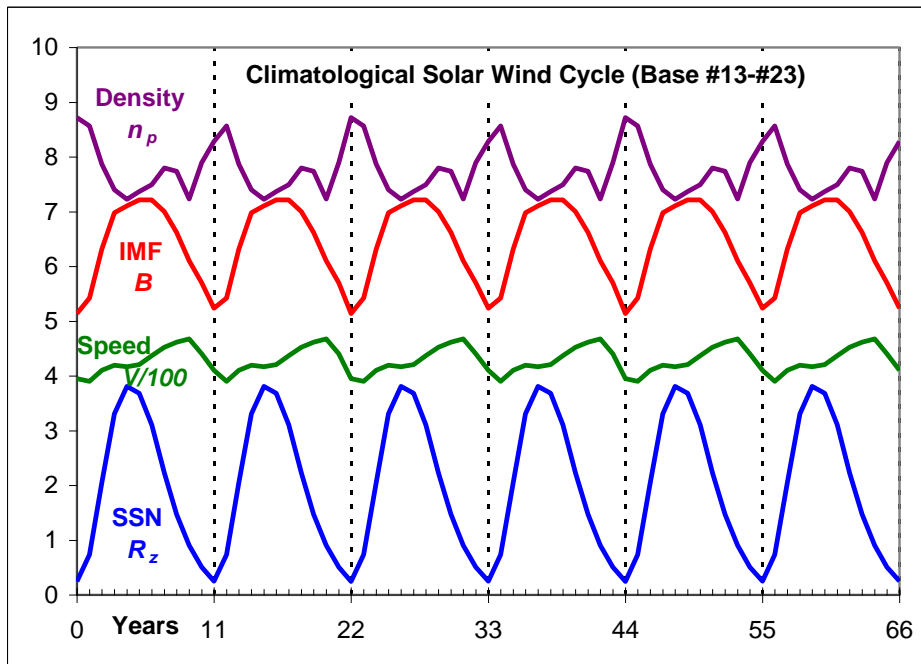
Determination of Solar Wind Density



The ratio between Magnetic Energy B^2 and kinetic energy nV^2 is found to depend slightly on the sunspot number R_z [Obridko et al.'s Quasi-invariant]

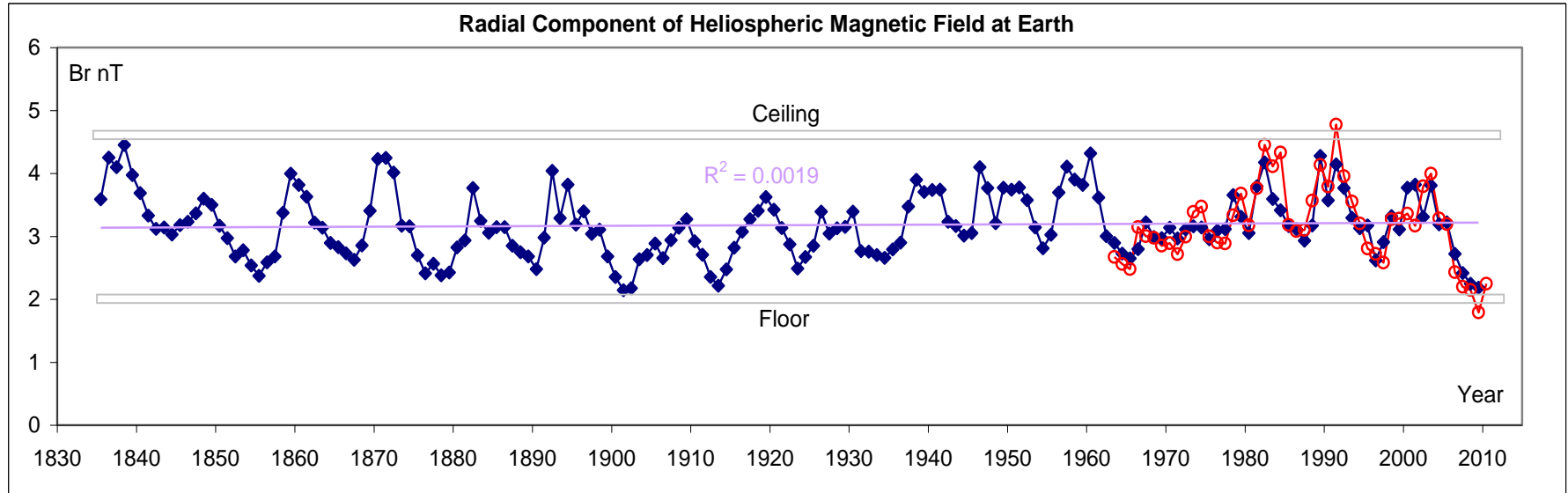
Pulling everything together we can construct the average solar cycle behavior of solar wind parameters from the 11 cycles for which we have good geomagnetic data.

Solar Wind Climate, if you will.



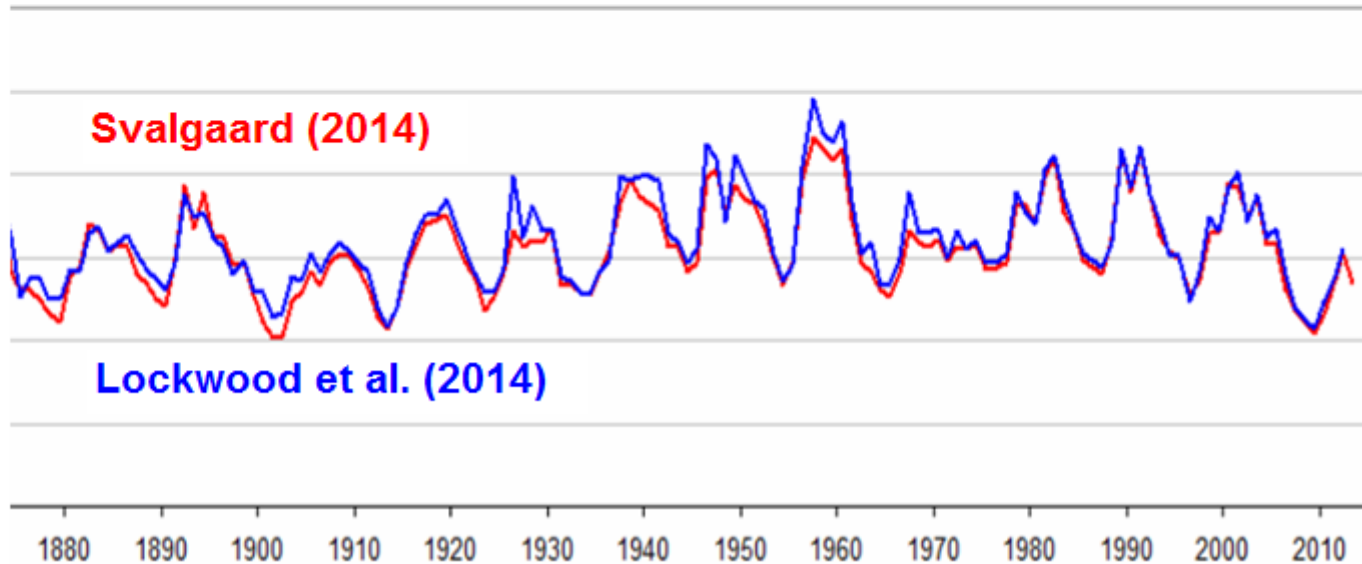
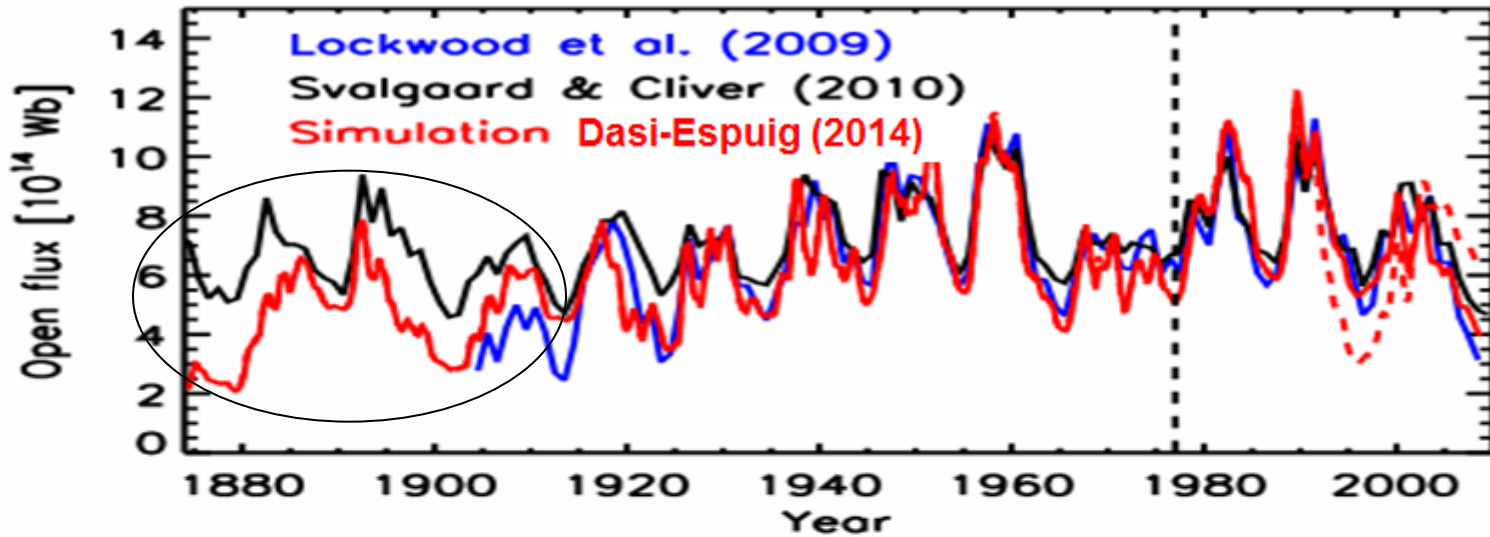
Radial Magnetic Field ('Open Flux')

Since we can also estimate solar wind speed from geomagnetic indices [IHV, Svalgaard & Cliver, JGR 2007] we can calculate the radial magnetic flux from the total B using the Parker Spiral formula:



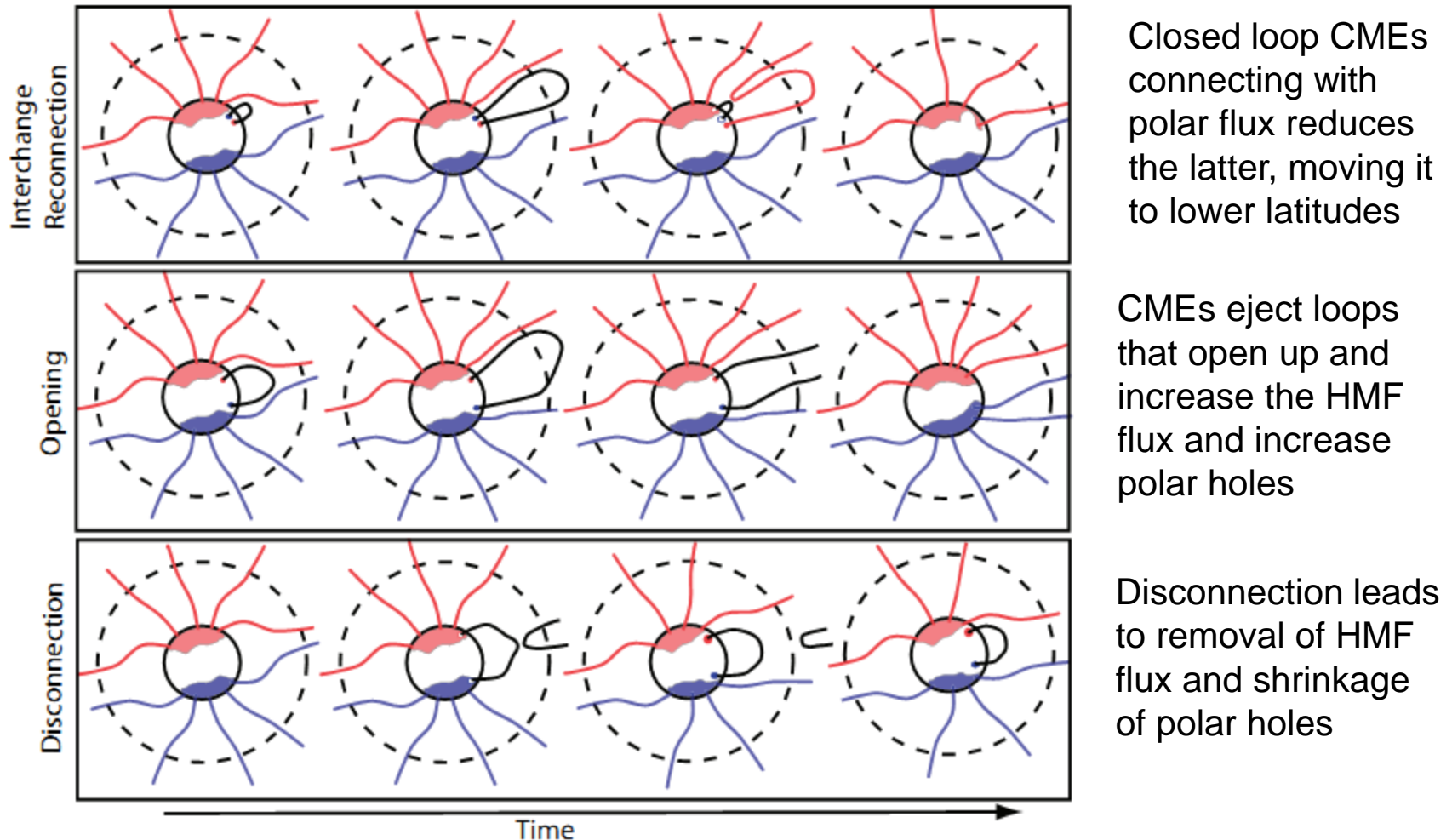
There seems to be both a Floor and a Ceiling and most importantly no long-term trend since the 1830s. Thus no Modern **Grand Maximum**.

Open Heliospheric Flux



Magnetic Flux Balance in the Heliosphere

Schwadron et al. ApJ 722, L132, 2010



Closed loop CMEs connecting with polar flux reduces the latter, moving it to lower latitudes

CMEs eject loops that open up and increase the HMF flux and increase polar holes

Disconnection leads to removal of HMF flux and shrinkage of polar holes

Determining Total Hemispheric Flux

The integral solution for the ejecta-associated [CME] magnetic flux is

$$\Phi_{ej} = \int_{-\infty}^t dt' \exp\left(-\frac{t-t'}{\tau_c}\right) f(t')(1-D)\phi_{CME}$$

Where the characteristic loss-time of the closed [CME] flux is

$$\frac{1}{\tau_c} = \frac{1}{\tau_{ic}} + \frac{1}{\tau_o} + \frac{1}{\tau_d}$$

And where the CME rate $f(t)$ is derived from the Sunspot Number SSN:

$$f(t) = SSN(t) / 25$$

The integral solution for 'open' heliospheric magnetic flux is

$$\Phi_0 = \Phi_{fir} + \int_{-\infty}^t dt' \exp\left(-\frac{t-t'}{\tau_d}\right) \frac{\Phi_{ej}}{\tau_o}$$

The total flux becomes $\Phi_{tot} = \Phi_0 + \Phi_{ej} = \oint \mathbf{B}_P \cdot \hat{n} dS = 4\pi R^2 |B_P|$

Which evaluated for $R = 1$ AU allows you to infer the HMF field strength, B , at Earth. The subscript P in B_P stands for the 'Parker Spiral Field'.

A Parameter Set Example

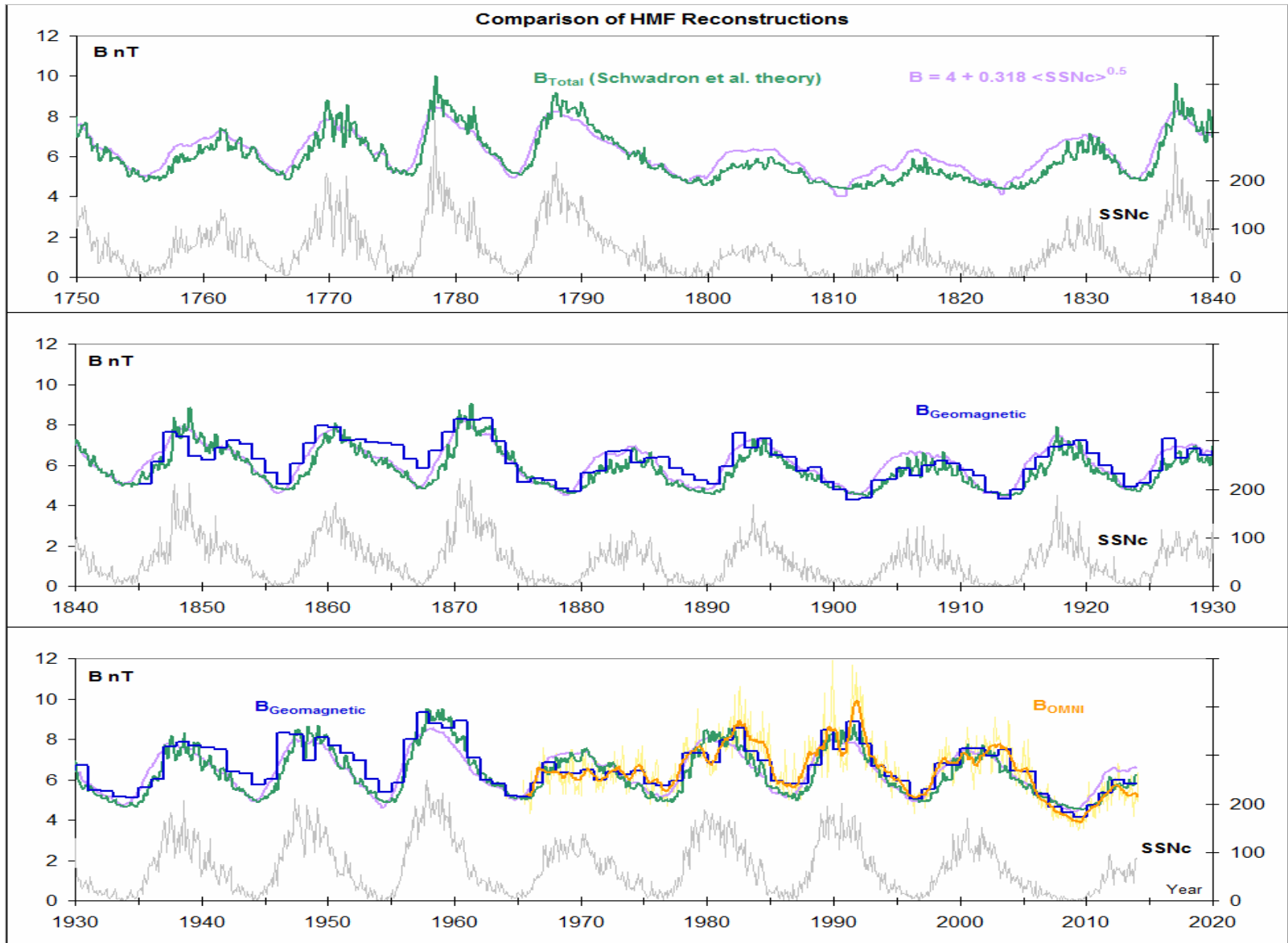
0.04	Number	Number of CMEs per day per unit sunspot number
15	Days	Timescale for interchange reconnection
4.0	Years	Timescale for opening of closed flux
3.0	Years	Timescale for loss of flux by disconnection
1	10^{13} Wb	Magnetic flux per CME
56	10^{13} Wb	Magnetic flux over whole sphere for a Floor in radial Br
0.6	Fraction	Fraction of flux closing on ejection
1.5	Factor	Factor to convert computed, ideal 'Parker' spiral B to messy, total B

von Neumann: *“with four parameters I can fit an elephant, and with five I can make him wiggle his trunk”*

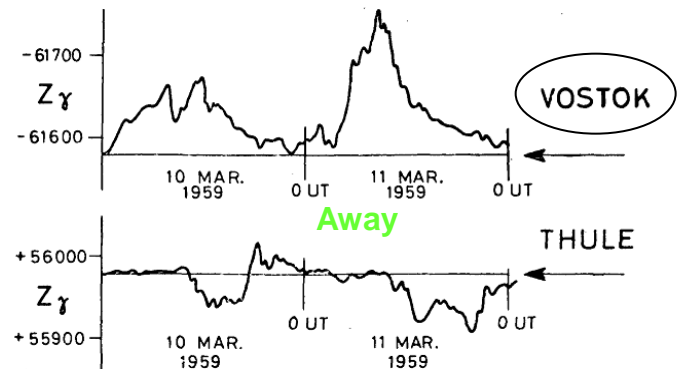
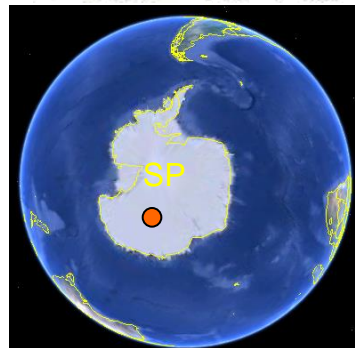
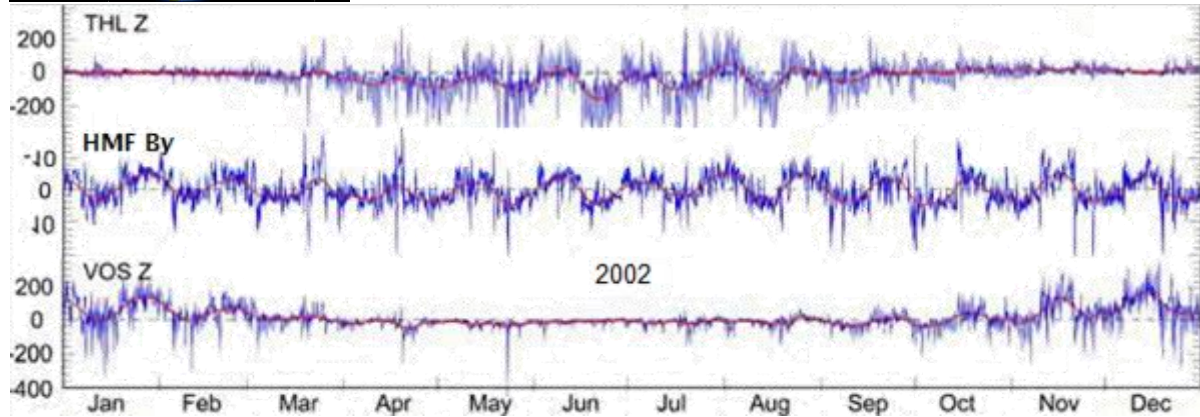
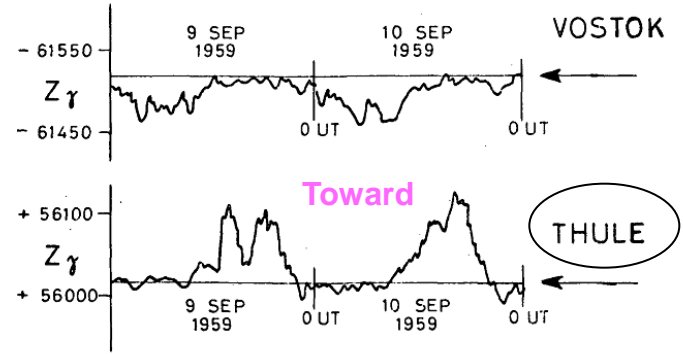
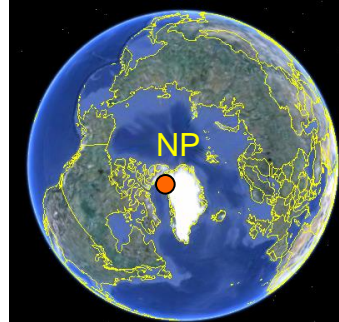
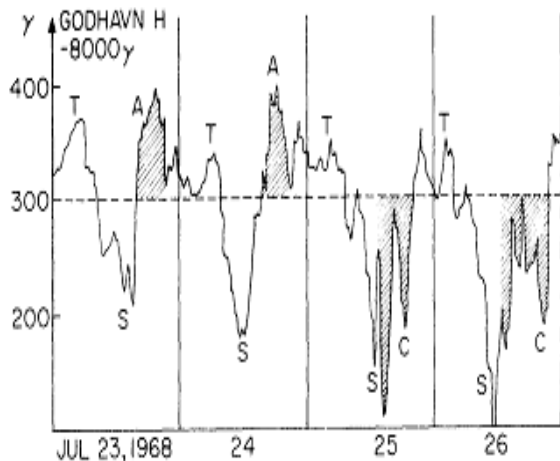
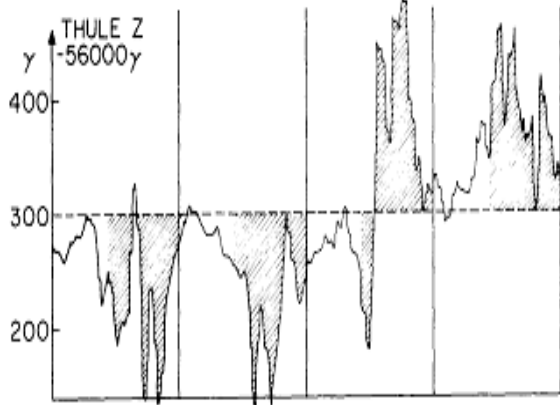
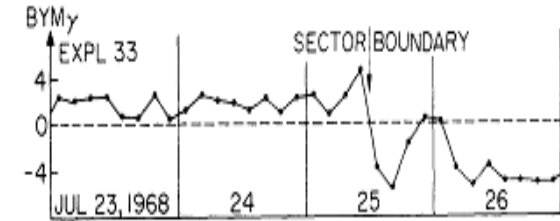
This model has about eight parameters...

So perhaps we can also make him wiggle both ears and the tail 😊

Schwadron et al. (2010) HMF B Model with my set of parameters

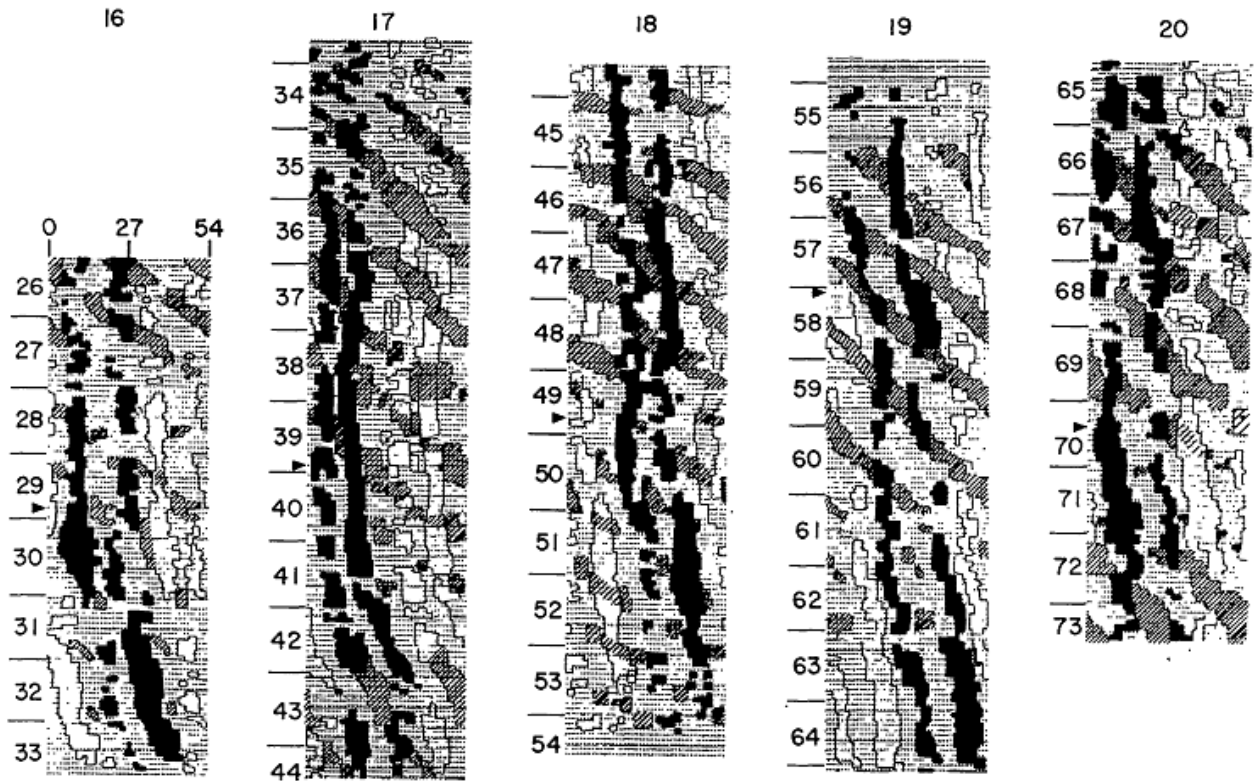
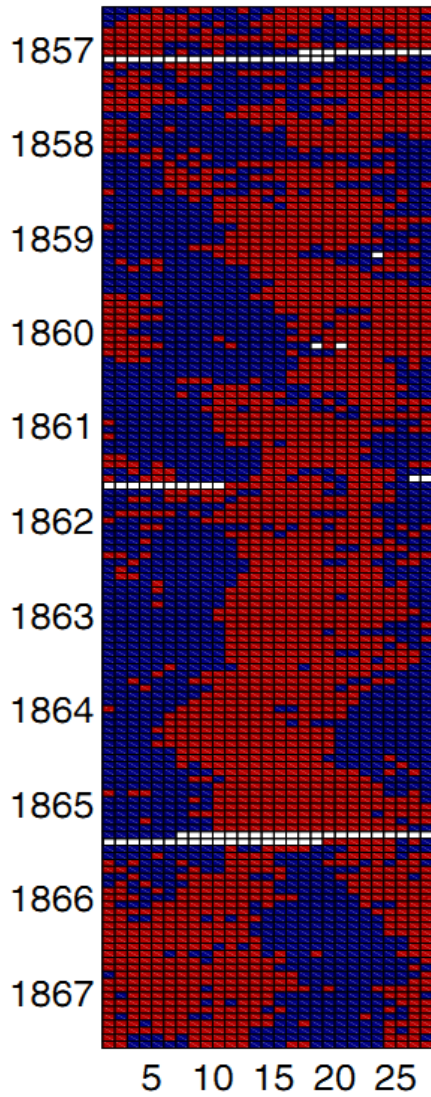


Svalgaard-Mansurov Effect



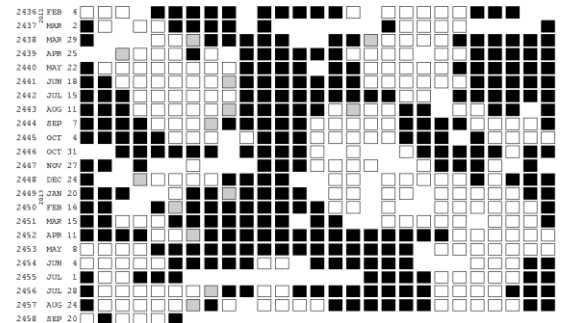
Not a subtle effect...

cycle 10



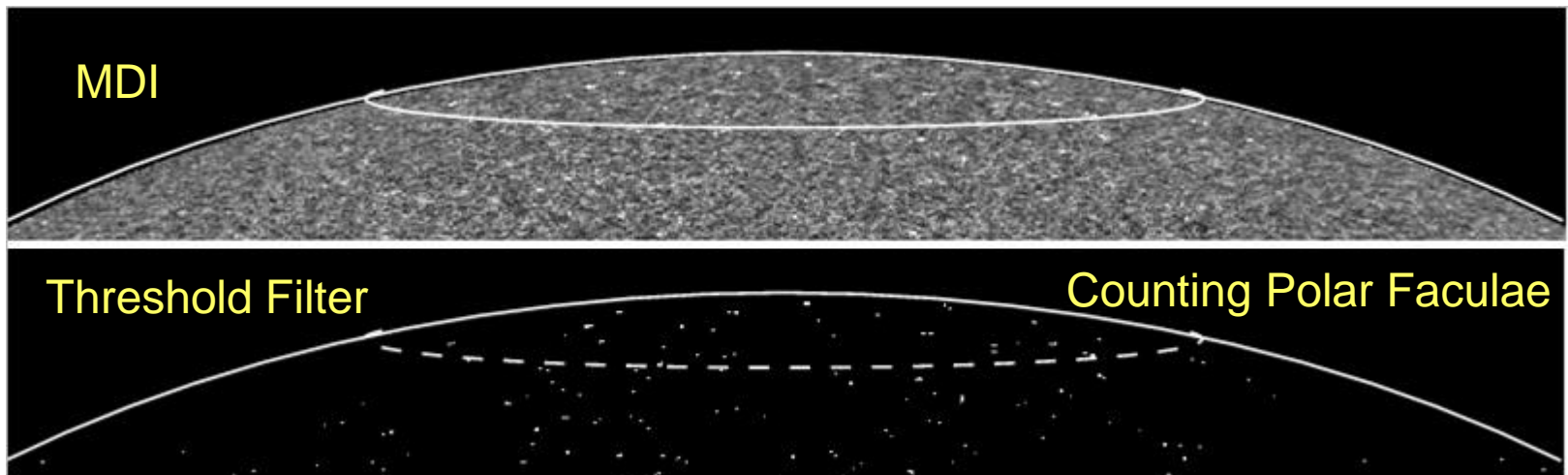
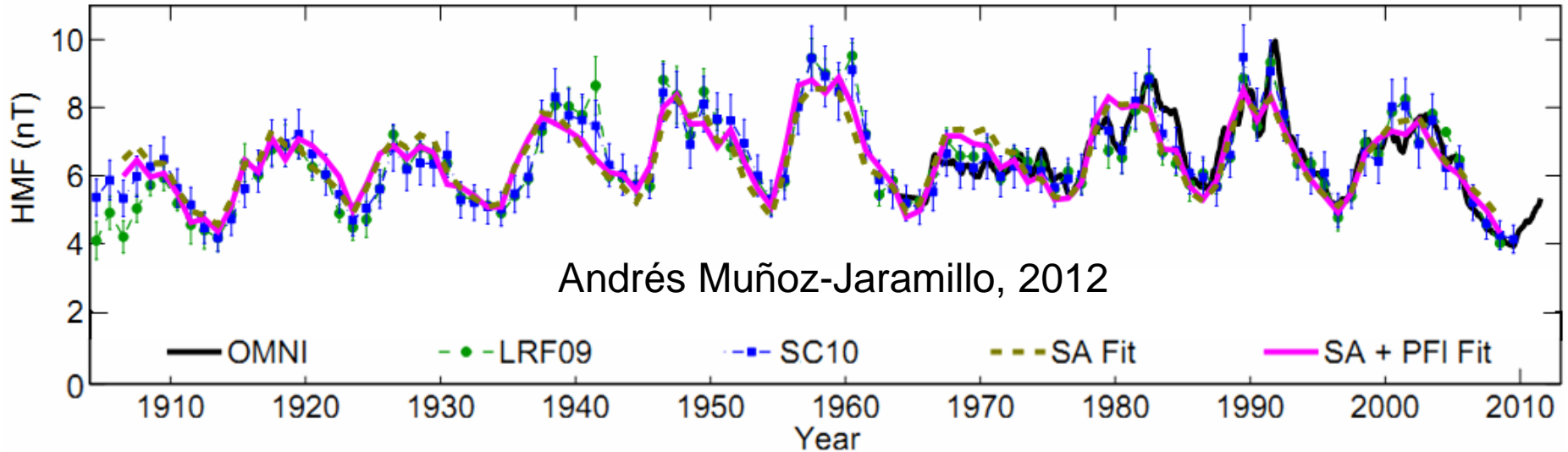
26.84 DAYS CALENDAR SYSTEM STARTING FEB 19, 1926

Sector Structure over Time



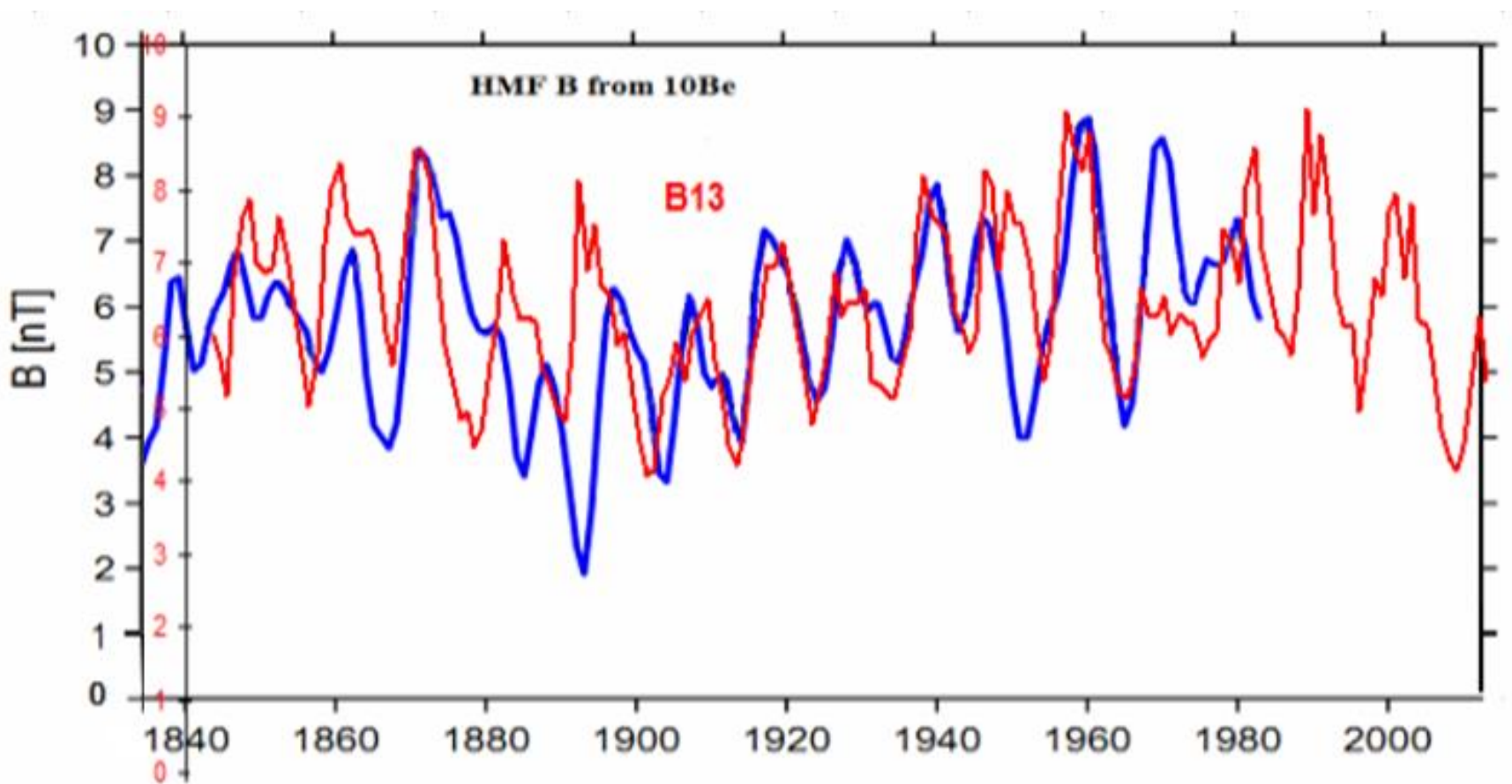
Vokhmyanin & Ponyavin, 2013

Combining Polar Faculae and Sunspot Areas can also give HMF B

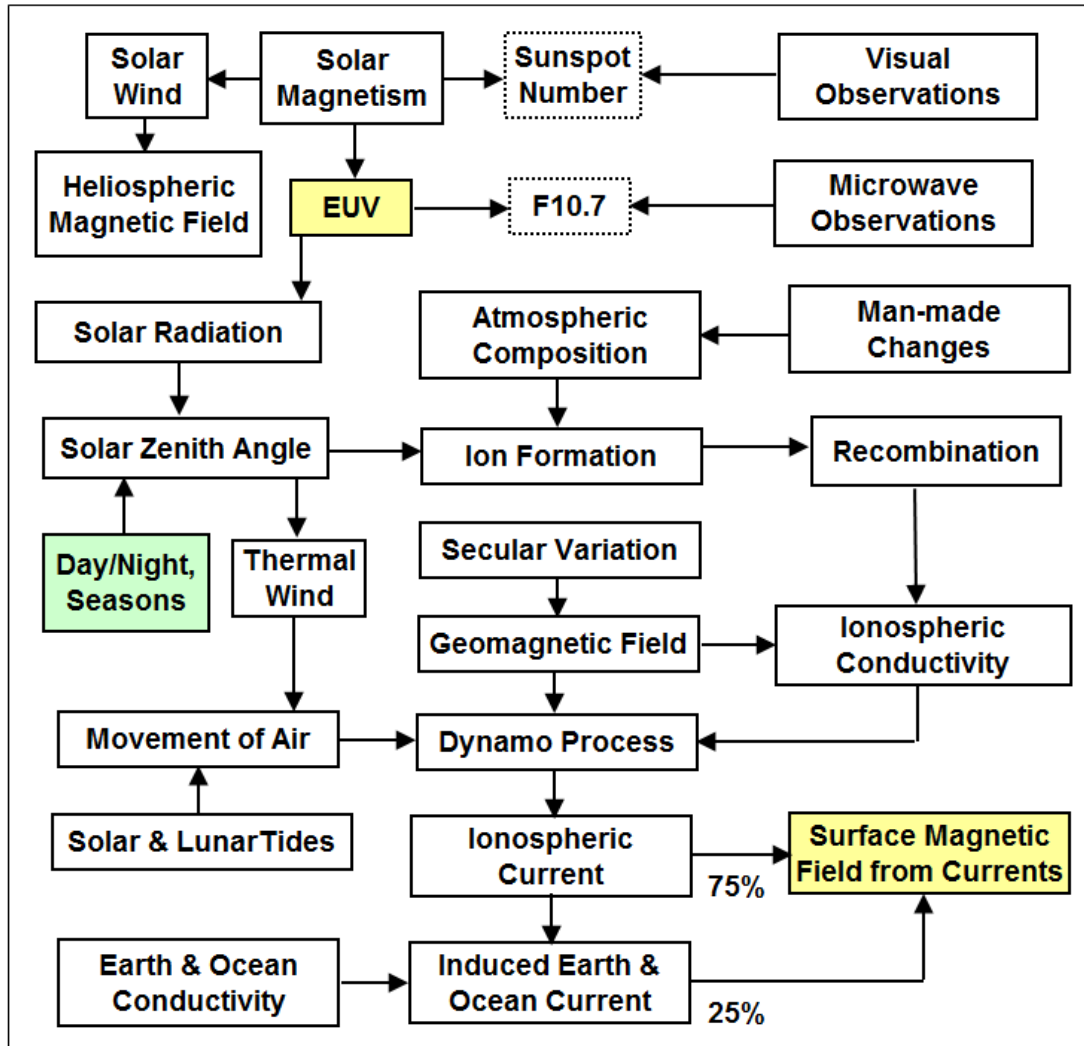


Re-evaluation of Cosmic Ray Data

Still problem with the 1880-1890s and generally with low values



The Effect of Solar EUV

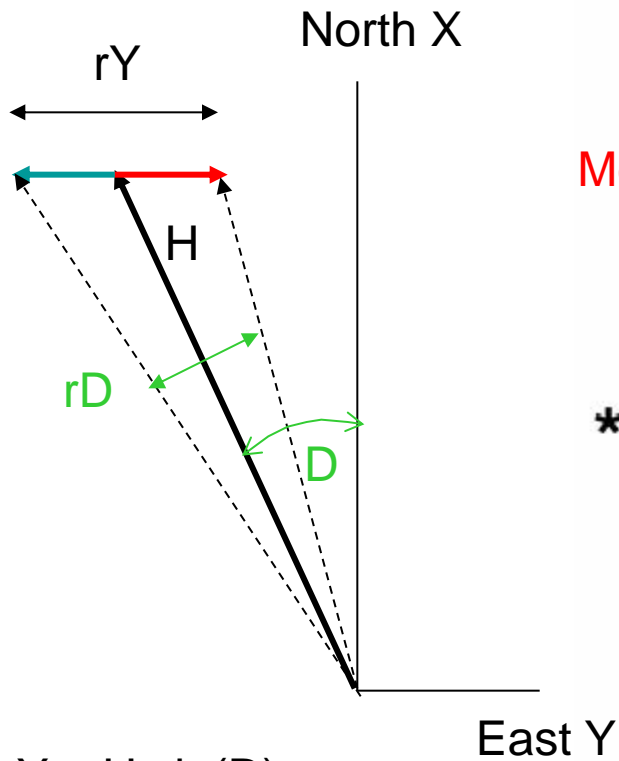
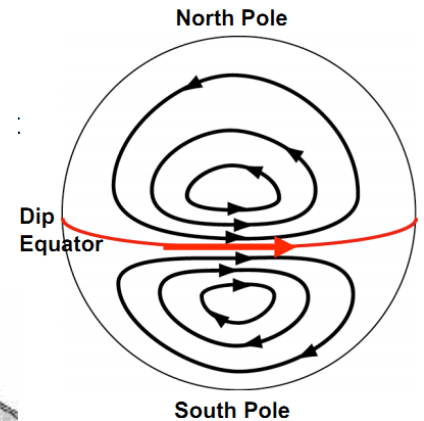


The EUV causes an observable variation of the geomagnetic field at the surface through a complex chain of physical connections.

The physics of each link in the chain is well-understood in quantitative detail and can be successfully modeled.

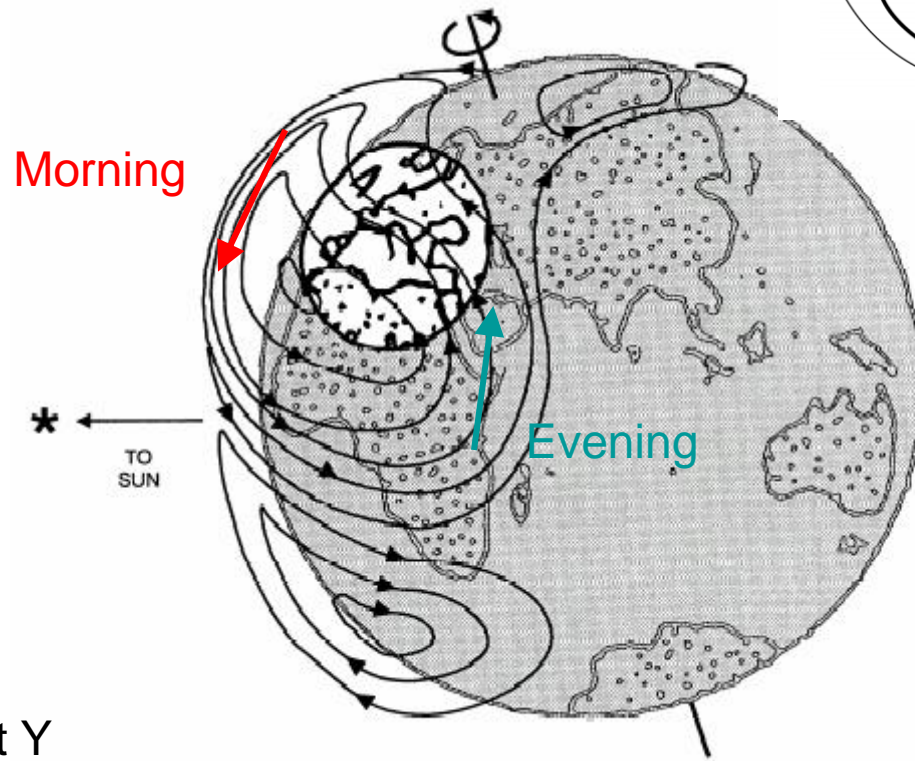
We'll use this chain in reverse to deduce the EUV flux from the geomagnetic variation.

The E-layer Current System



$$Y = H \sin(D)$$

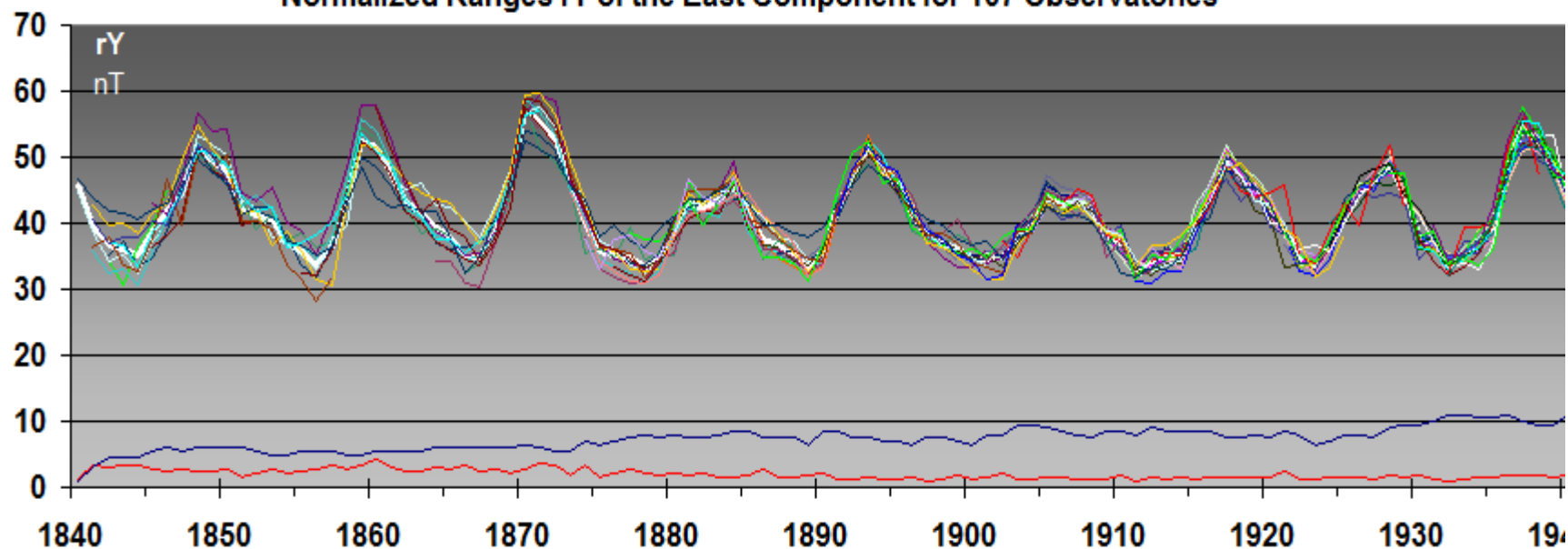
$$dY = H \cos(D) dD \text{ For small } dD$$



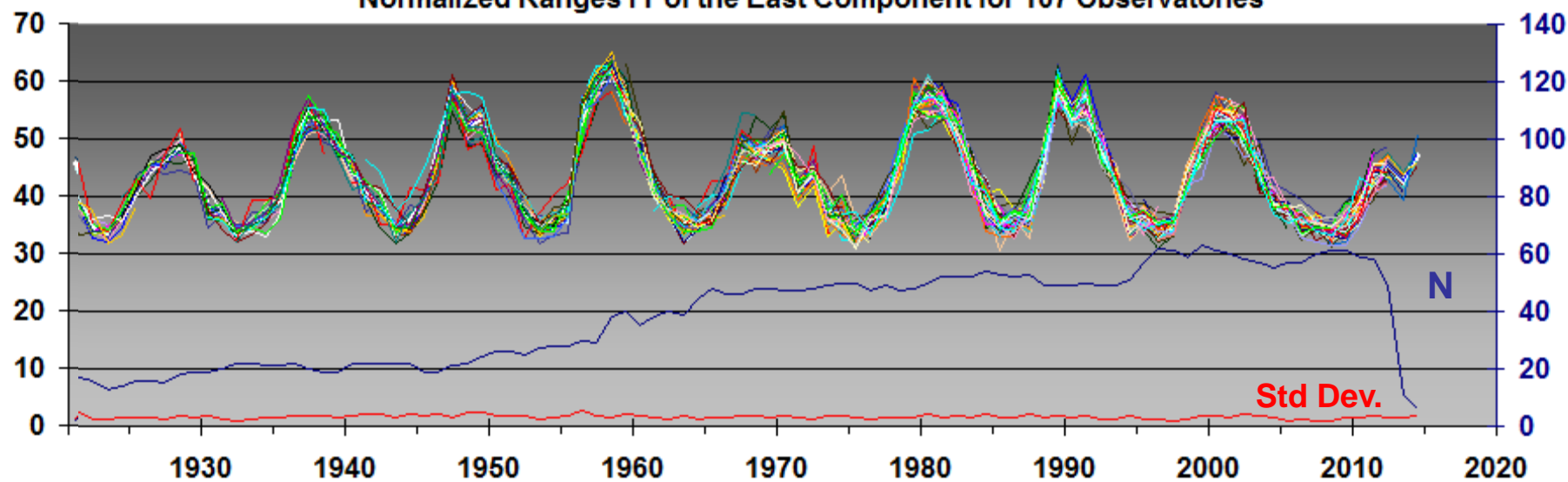
A current system in the ionosphere is created and maintained by solar EUV radiation

The magnetic effect of this system was discovered by George Graham in 1722

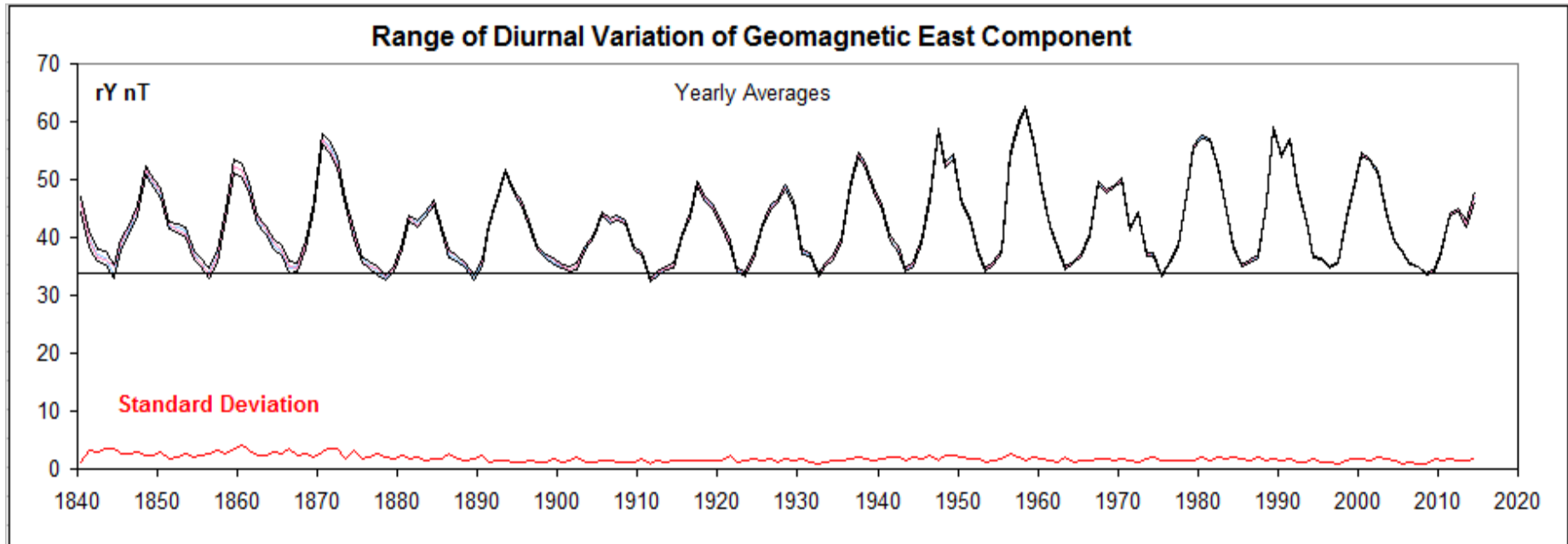
Normalized Ranges rY of the East Component for 107 Observatories



Normalized Ranges rY of the East Component for 107 Observatories



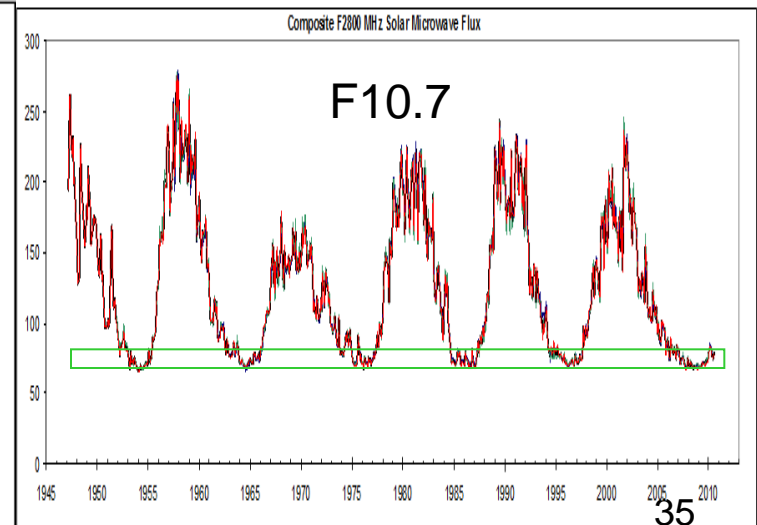
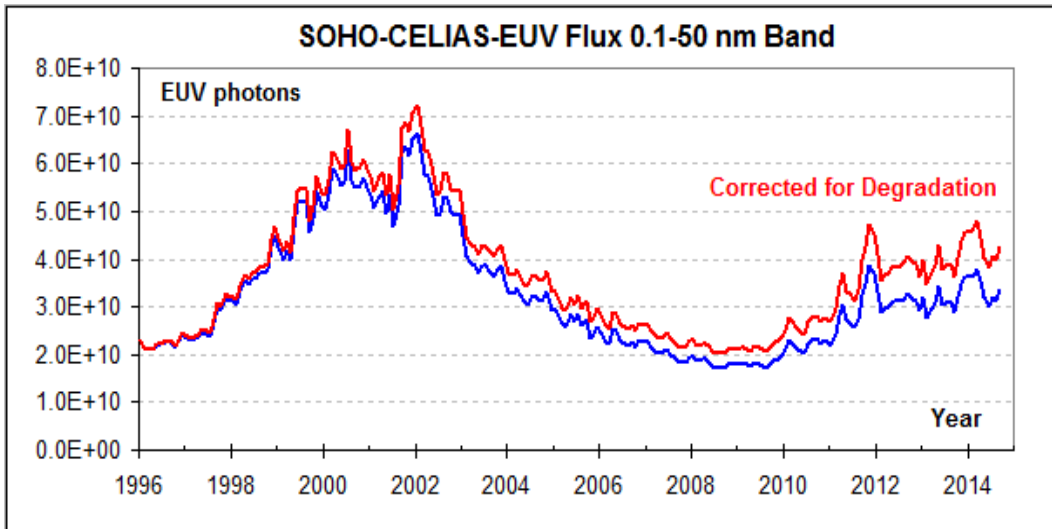
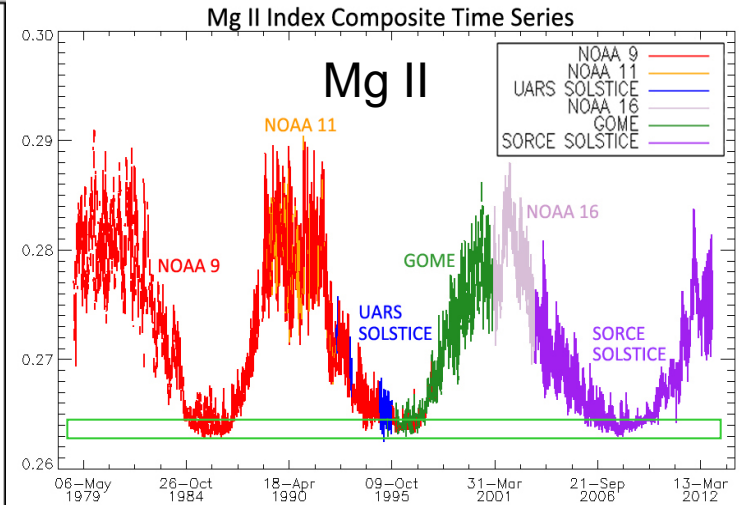
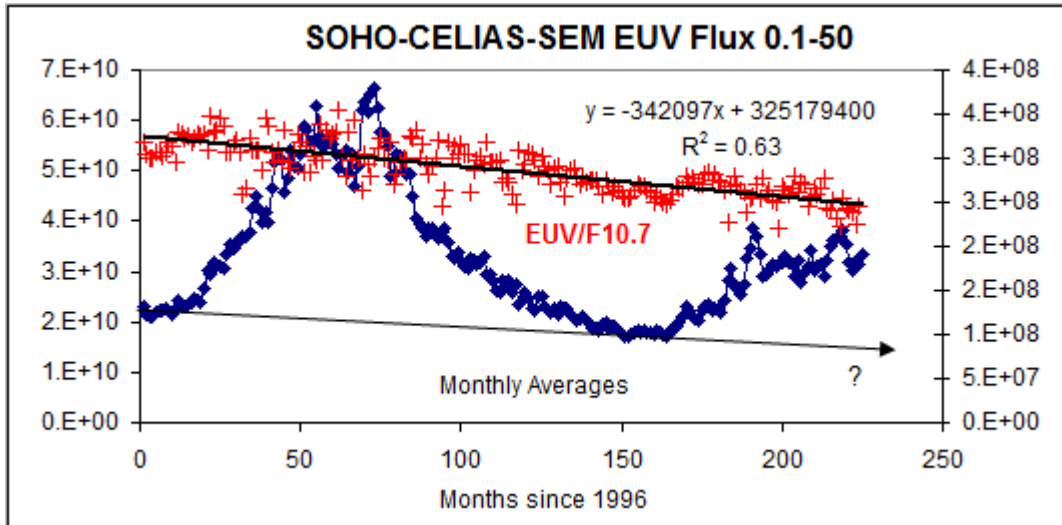
Composite rY Series 1840-2014



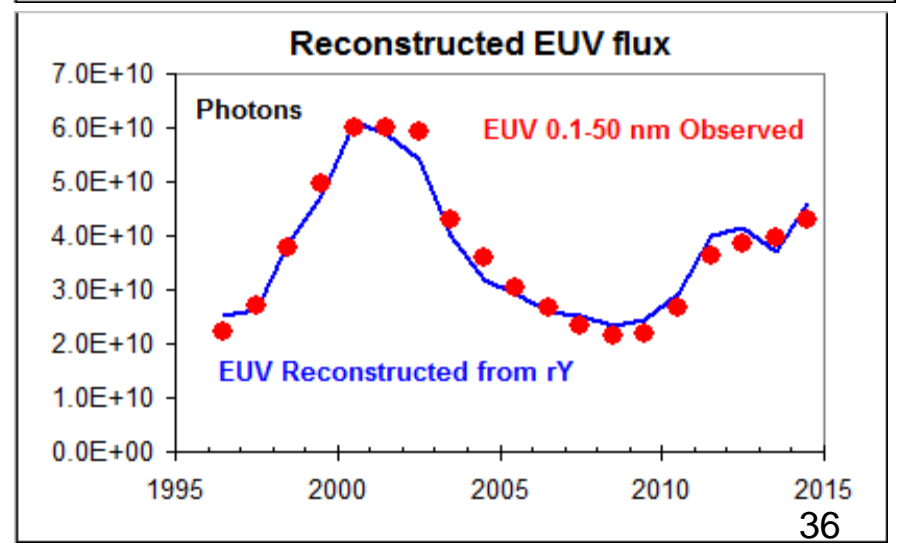
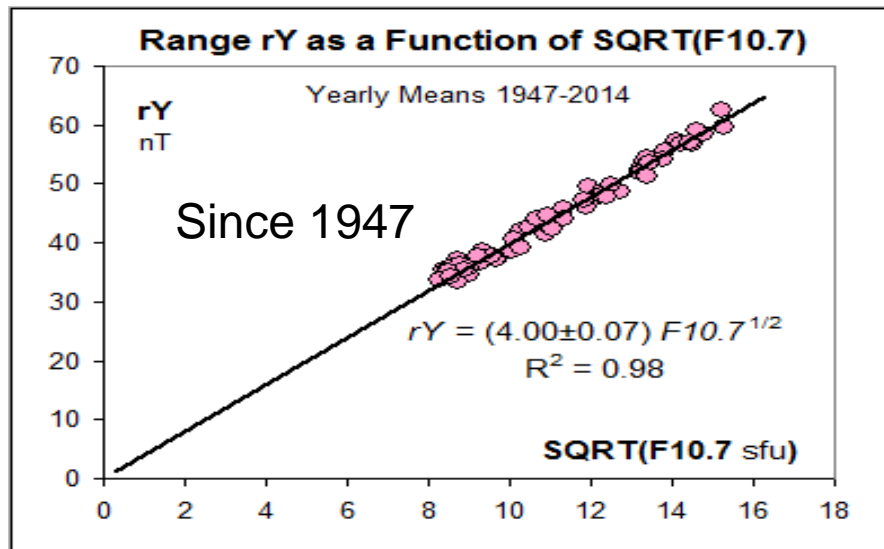
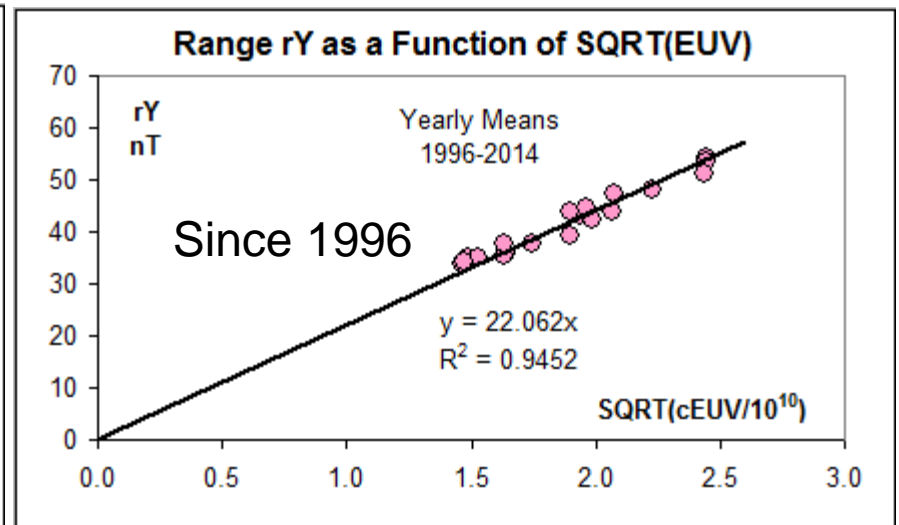
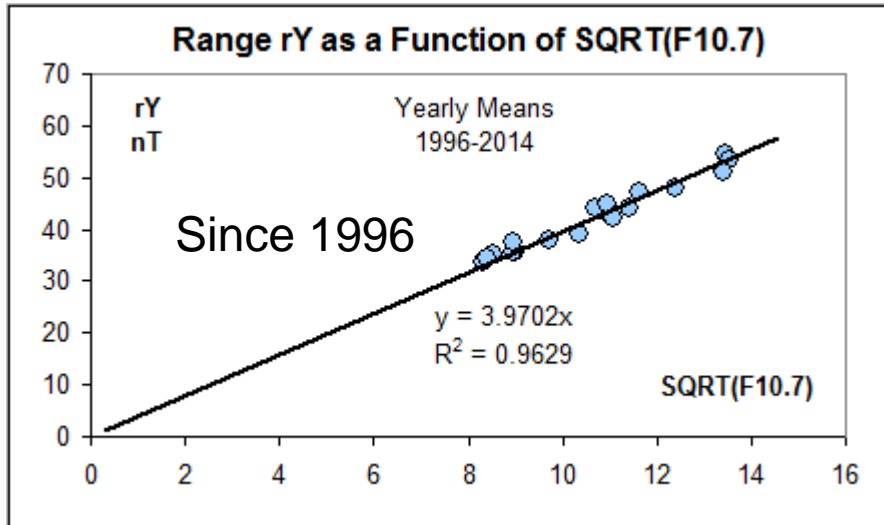
From the Standard Deviation and the Number of Station in each Year we can compute the Standard Error of the Mean and plot the ± 1 -sigma envelope

Since the ionospheric conductivity, Σ , depends on the number of electrons N , we expect that Σ scales with the square root of the overhead EUV flux (the Chapman function: $N = \sqrt{J/\alpha \cos(\chi)}$, J = ionization rate, α = recombination rate, χ = Zenith angle for the dominant plasma species O^+_{2} for $\lambda < 102.7$ nm)

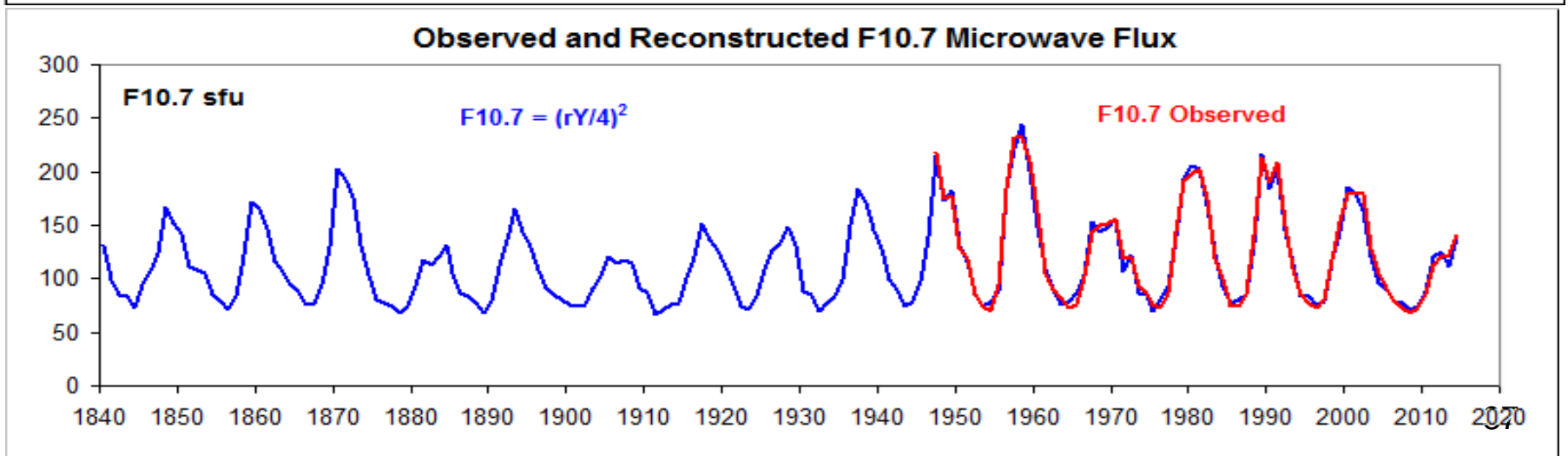
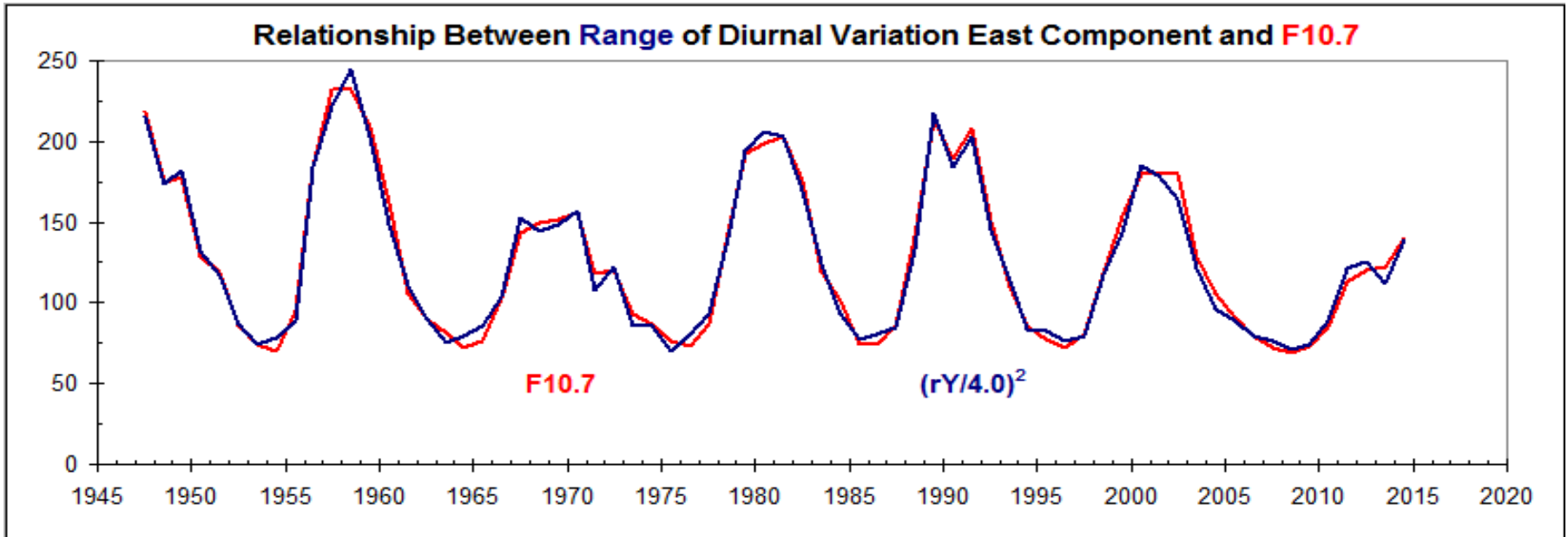
Correcting the SEM-series for Degradation Comparing with F10.7 and Mg II Indices



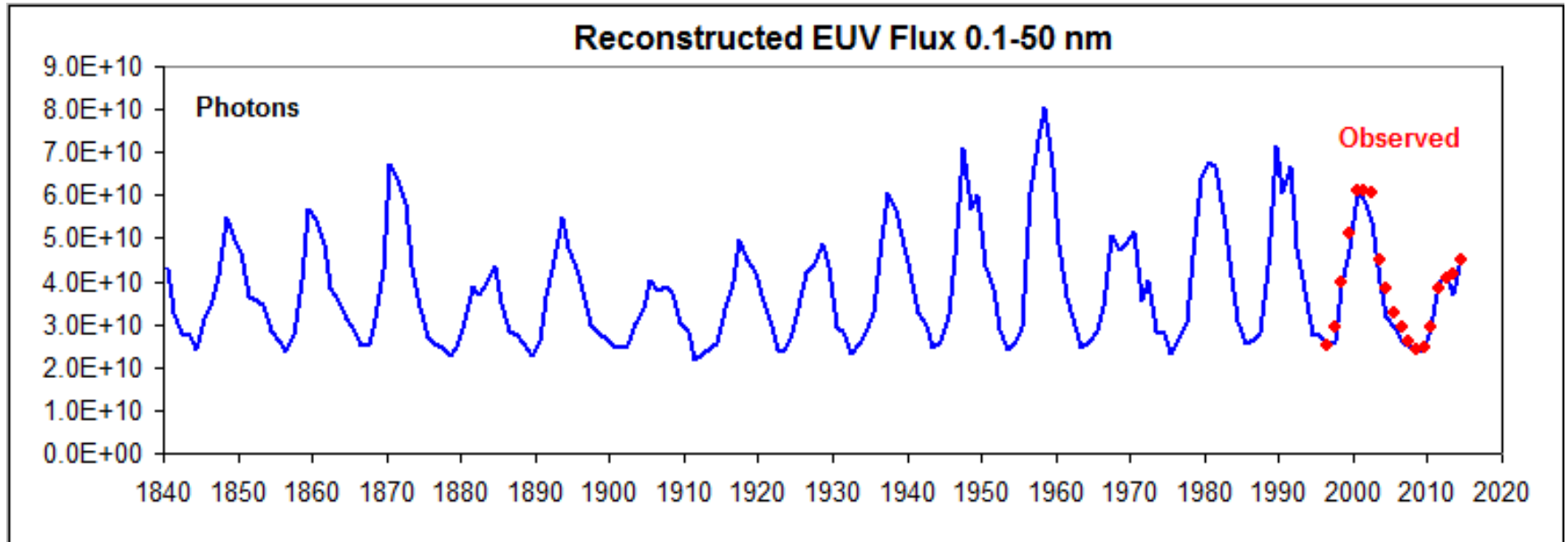
rY and $F10.7^{1/2}$ and $EUV^{1/2}$



Reconstructed F10.7 [an EUV Proxy]

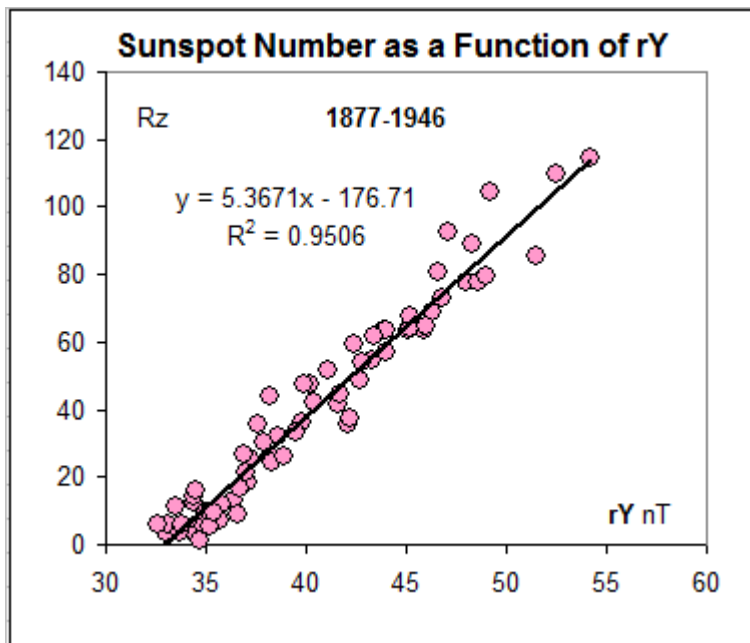


Reconstructed EUV Flux 1840-2014



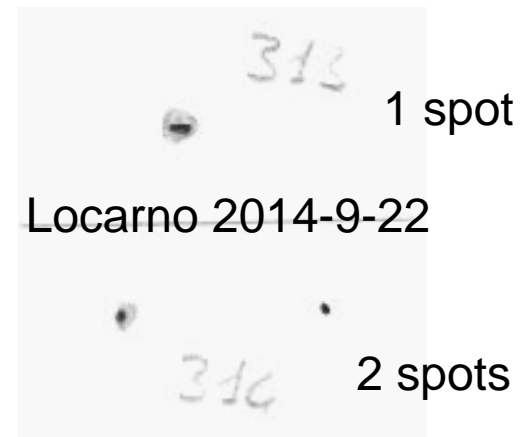
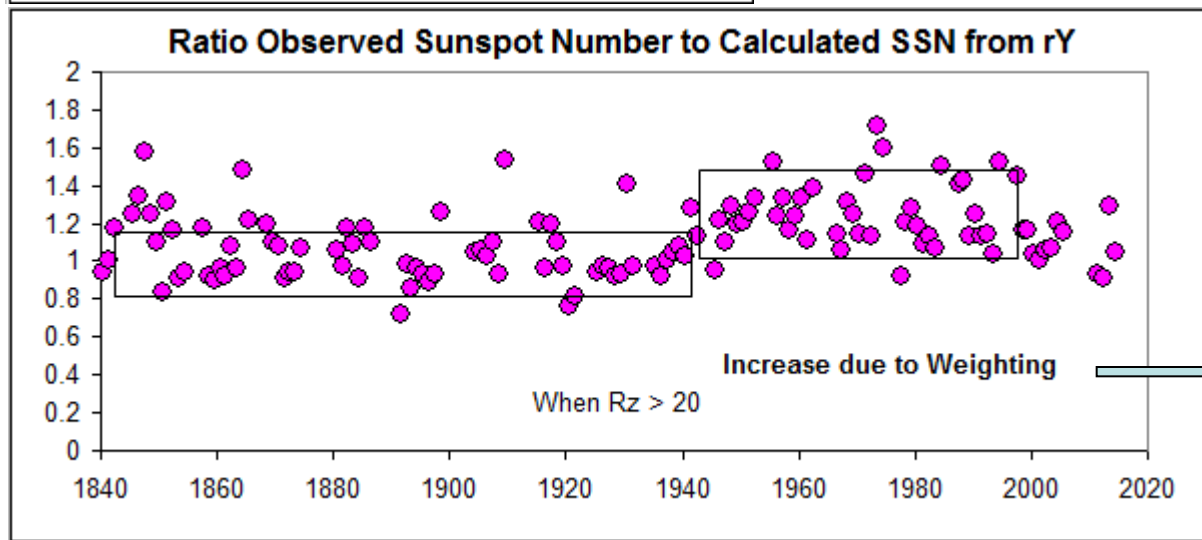
This is, I believe, an accurate depiction of true solar activity since 1840

We can compare that with the Zurich Sunspot Number



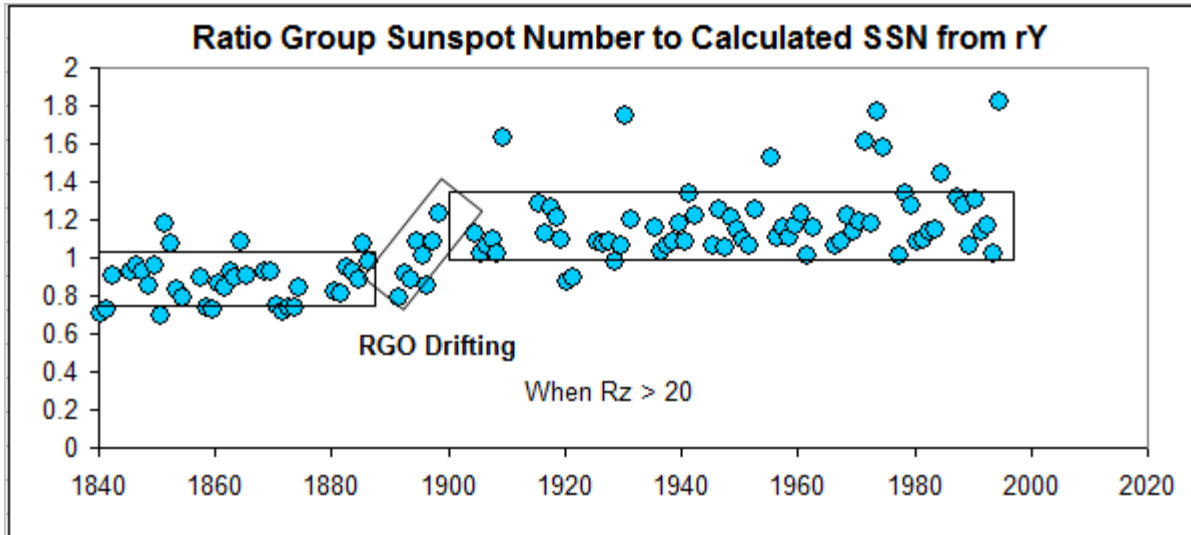
	ratio
1840-1876	1.052
1877-1946	1.000
1947-1999	1.210
2000-Now	1.022

Wolfer & Brunner

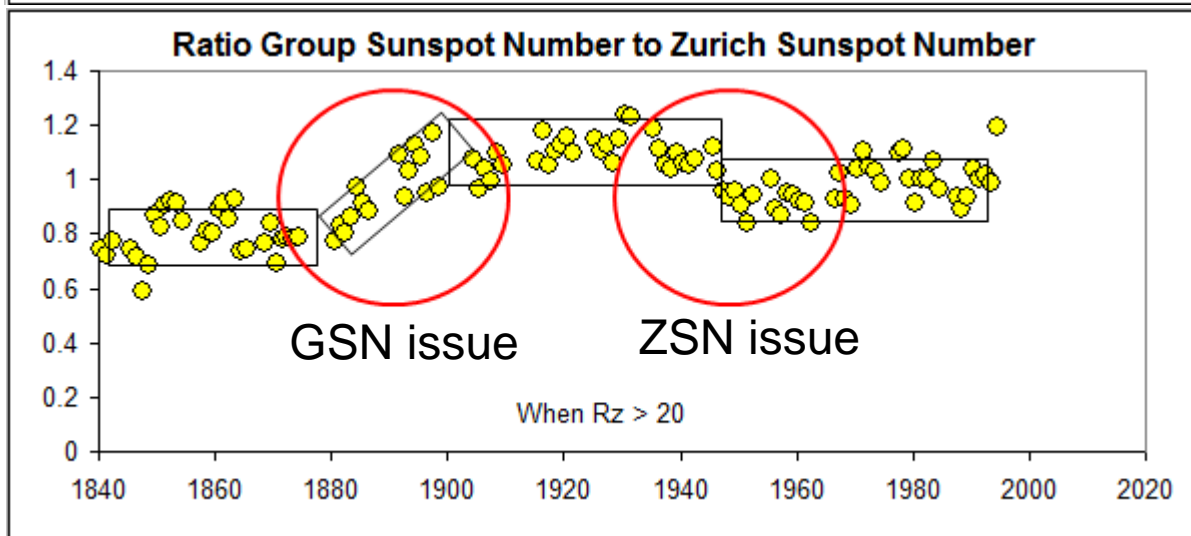


g	f	t	B
313	3	J	+11'
316	4	C	+5'

How About the Group Sunspot Number?

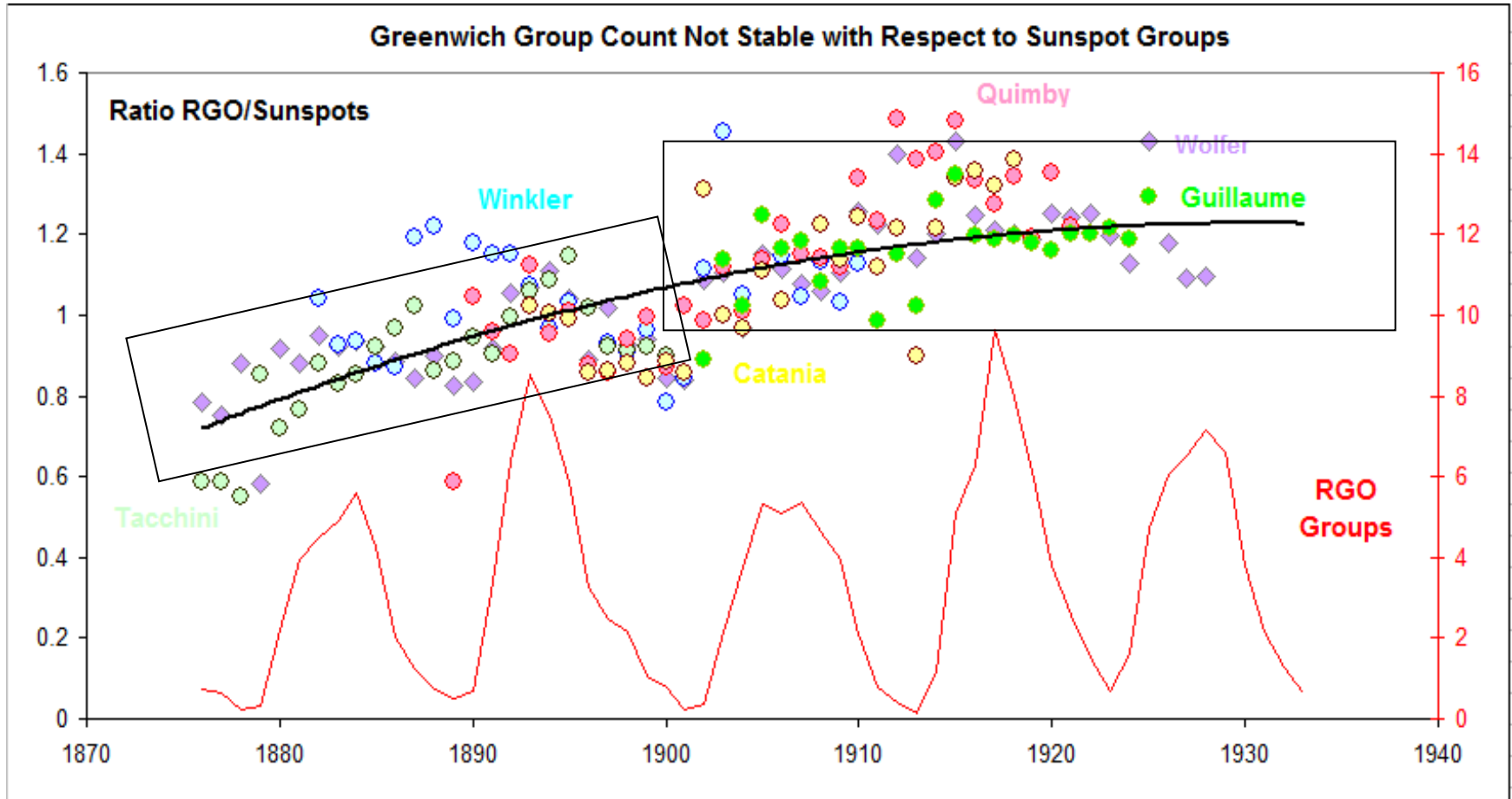


The main issue with the GSN is a change relative to the ZSN during 1880-1900. This is mainly caused by a drift in the reference count of the standard (Royal Greenwich Observatory)



The ratio between the Group Sunspot Number reveals two major problem areas. We can now identify the cause of each

RGO Groups/Sunspot Groups



Early on RGO counts fewer groups than Sunspot Observers



Sunspot 2011



Brussels 2012



Tucson 2013

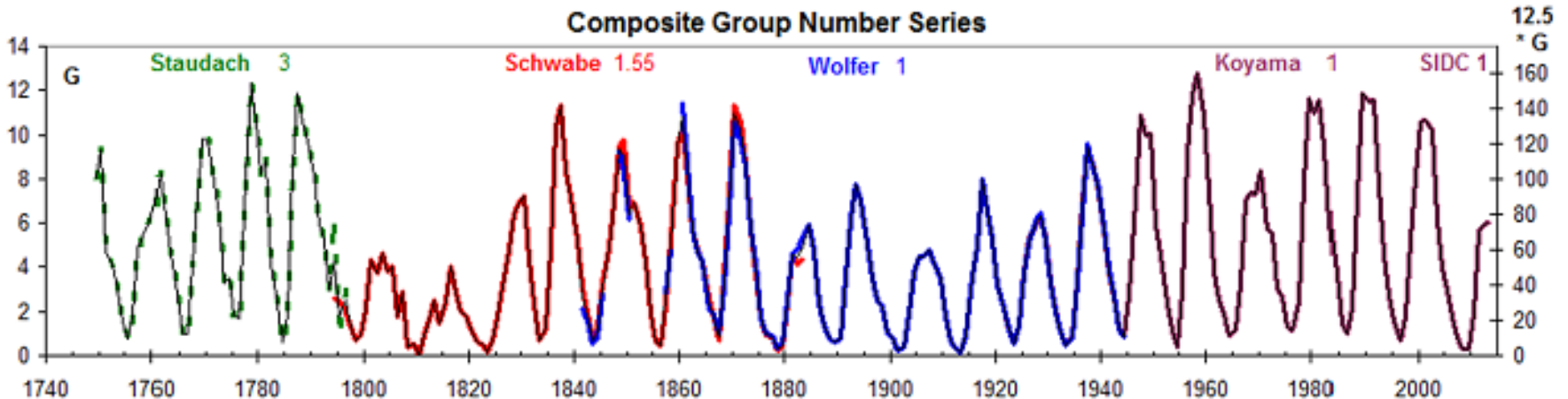


Locarno 2014

The SSN Workshops

A series of workshops have led to a critical re-assessment of the Sunspot Number series: Clette et al., Space Science Reviews, 2014

An official revised series is scheduled for 2015



High solar activity in every century since 1700. None stand out as **Grand**

Abstract

Over the past decade there has been significant progress in the study of solar variability on the time scale of centuries. New reconstructions of Sunspot Numbers, Extreme Ultraviolet and Microwave proxies, Solar Wind Physical Parameters, Total Solar Irradiance, Solar Polar Fields and Cosmic Ray Modulation have provided a well-constrained and consistent consensus of solar variability over the past two centuries. The new insights promise further progress in modeling solar activity much further back in time.